CHALMERS
UNIVERSITY OF TECHNOLOGY

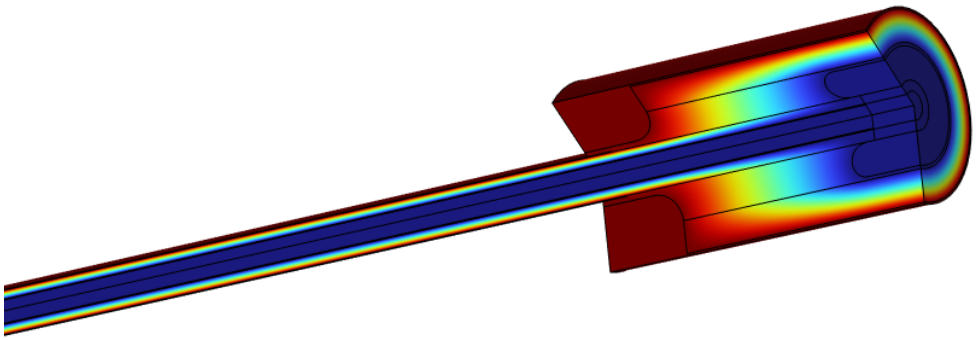

TESTING OF FIELD GRADING MATERIALS FOR HVDC CABLE JOINTS

Master's thesis in Electric Power Engineering

SAJIL KAPPADAN

DEPARTMENT OF ELECTRICAL ENGINEERING

CHALMERS UNIVERSITY OF TECHNOLOGY
Gothenburg, Sweden 2025
www.chalmers.se

Master's thesis in Electric Power Engineering 2025

TESTING OF FIELD GRADING MATERIALS FOR HVDC CABLE JOINT

SAJIL KAPPADAN

CHALMERS
UNIVERSITY OF TECHNOLOGY

Division Of Electric Power Engineering
Department Of Electrical Engineering
Chalmers University of Technology
Gothenburg, Sweden 2025

TESTING OF FIELD GRADING MATERIALS FOR HVDC CABLE JOINTS

Supervisors: Susanne Nilsson, Head Of R&D at NKT;
Rashid Hussain, Senior High Voltage Specialist at NKT;
Sajjad Jafari, Junior High Voltage Specialist at NKT;
Jenny Hedlund, Material Specialist at NKT.

Examiner: Prof. Yuriy Serdyuk, Chalmers University of Technology

Master's Thesis 2025
Department of Electrical Engineering
Division of Electric Power Engineering
Chalmers University of Technology
SE-412 96 Gothenburg
Telephone +46 31 772 1000

Cover:3D Visualization of a High Voltage Direct Current (HVDC) Cable Joint using COMSOL.

Gothenburg, Sweden 2025

TESTING OF FIELD GRADING MATERIALS FOR HVDC CABLE JOINTS

SAJIL KAPPADAN
Department of Electrical Engineering
Division of Electric Power Engineering
Chalmers University of Technology

Abstract

HVDC cable systems are designed to transmit large amounts of electricity over long distances with minimal losses. Most failures in these systems happen because of issues with cable accessories like joints and terminations. They are caused by strong electric fields appearing in such components due to geometrical features of the designs and inhomogeneities in the structure of the insulation system incorporating various materials. To enhance the performance of cable accessories, electric field control in the insulation is crucial. To address this, so-called field grading materials (FGMs) can be used to even out the electric field distributions. Thanks to their non-linear properties, these materials secure normal operations of the cable system and also are capable of handling events like lightning overvoltage and switching impulses.

This thesis focuses on exploring electrical and mechanical properties of FGMs by testing samples of materials with different types and concentration of fillers at various temperatures and electric field strength. The focus is on a comparative analysis, where the properties of EPDM (Ethylene Propylene Diene Monomer) are taken as a reference. New materials with good electrical and mechanical properties are selected based on specific criteria, followed by measurements of their non-linear conductivity. Experimental results show that three selected materials met the criteria for nonlinear conductivity. To further evaluate their performance as a base for building a large scale component, electrothermal simulations of a 525 kV DC cable joint made of those materials have been conducted for different voltage levels including nominal, type test and lightning impulse voltages. The simulation results show minimal differences in the field grading effects caused by the selected FGMs applied in different locations of the cable joint, likely because of similar non-linear behavior of their properties in the studied ranges of temperatures and electric stresses.

Acknowledgements

I am deeply grateful to several individuals whose support and guidance have been crucial to the completion of this thesis.

First and foremost, I would like to extend my heartfelt thanks to my manager at NKT, Susanne Nilsson, for selecting me for this thesis project. Her trust in my abilities and encouragement throughout this journey have been greatly appreciated.

I am also profoundly grateful to my supervisors at NKT, whose contributions have been indispensable. Dr. Rashid Hussain provided invaluable support with the theoretical and simulation aspects of my research. Sajjad Jafari taught me the electrical testing procedures and offered insightful guidance in clearing my doubts, which was essential to my progress. Jenny Hedlund was instrumental in the sample preparation and mechanical properties testing, ensuring the reliability and accuracy of my results.

Finally, I wish to express my sincere gratitude to Professor Yuriy Serdyuk for his comprehensive guidance and mentorship throughout the entire process. His expertise and support have been pivotal in shaping the direction and success of this thesis.

Thank you all for your exceptional support, patience, and dedication.

Sajil Kappadan, Gothenburg, July 2024

List of Acronyms

Below is the list of acronyms that have been used throughout this thesis listed in alphabetical order:

HVDC	High Voltage Direct Current
FGM	Field Grading Material
EPDM	Ethylene Polymer Diene Monomer
LSR	Liquid Silicone Rubber
PV	Photovoltaic
RES	Renewable-based Energy Sources
EHV	Extra High Voltage
PDC	Polarisation and Depolarisation Current
SiC	Silicon Carbide
ZnO	Zinc Oxide

Contents

List of Figures

List of Tables

1

Introduction

This master thesis explores the testing of Field Grading Materials (FGMs) to introduce these materials in to High Voltage cable accessories such as cable joints and terminations. More specifically, the main aim of this thesis is to perform the electrical testing of FGMs such as electrical conductivity, permittivity, dielectric losses and AC breakdown test, and some of the mechanical tests are also to be investigated. This master thesis is offered by the leading high voltage cable manufacturing company "NKT" which was established in 1891 and grown among 16 countries. Usually, the largest sustainable electrical sources like offshore wind farms are located far remote from the main users and one of the biggest challenges is how to transmit this high level of energy with minimal losses. To overcome this challenge, DC is preferred over AC. NKT has long experience in HVDC products, such as cables and cable accessories, where these accessories are produced in NKT's location Alingsås.

One type of material that can be used in HVDC accessories is FGM. This thesis work explores the impact of varying content of both field grading fillers and other fillers on critical properties such as non-linear DC conductivity and mechanical properties. Lab work was performed at NKT R&D lab in Alingsås. And then electrical tests under different scenarios have to be investigated to know the impact of corresponding FGM on the electric field distribution within the joint.

1.1 Background

HVDC cable systems are used globally for transmitting large amount of power across extensive distances, particularly in cases where HVAC connections are either impractical or unfeasible. In Europe, HVDC connections primarily serve as inter connectors within the Mediterranean region and are utilized for both inter connection purposes and linking offshore wind farms in the North sea. Presently, the highest voltage level frontier for submarine projects starts at 600 kV. whereas, the majority of projects are operating at 525 kV [1].

The main cause of failure in cable system is not the cable itself, but rather the malfunction of cable accessories. More than 70 % cable system failure can be attributed to issues with these accessories [1]. Thus, the proper design of cable accessories has to be done to improve the efficiency of cable systems. Figure 1.1 provides a visual representation of failure data for EHV cables [1].

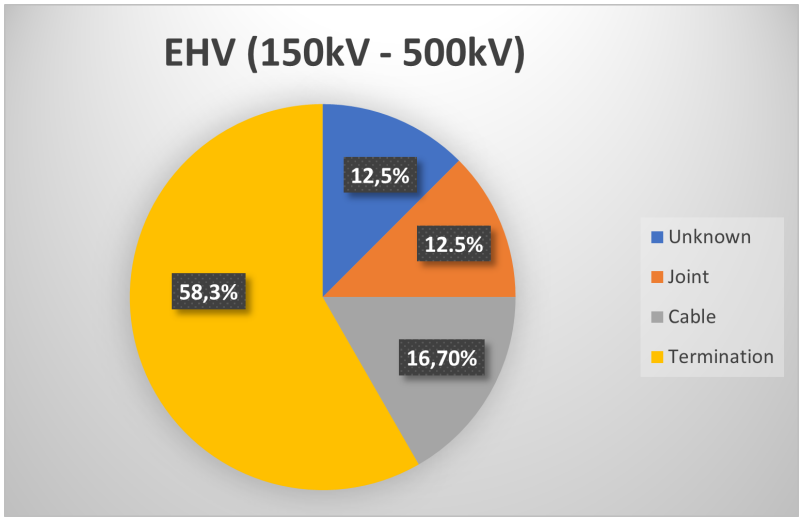

Figure 1.1: Illustration of cable system failure of EHV cables [1]

Field Grading Materials (FGMs) in HVDC cable joints refers to specialized materials used to manage electric field distribution within the joint structure. These materials can be used in HVDC systems where high voltages are transmitted over long distances, as they help to mitigate issues such as electrical stress concentration and partial discharge which can lead to joint failure .

In HVDC cable joints, field grading materials typically consist of special particles dispersed within an insulating polymer matrix. These materials are strategically placed within the cable joint to ensure more uniform distribution of electric field, reducing the risk of localized high- stress areas and improving the overall performance of joint.

1.2 The problem being addressed

This thesis will helps to investigate the properties (both electrical and mechanical) of field grading materials, when changing the filler shape, filler concentrations, electric field strength and temperature range.

1.3 Purpose

The main purpose of this thesis is to perform the experimental study on the different FGMs under varying electric fields and temperatures. The experimental study mainly focusing on the electrical testing . However, some of the mechanical tests has to be done. These tests are small scale tests and thus test samples with 1mm thickness are considered for the electrical testing and 2 mm for the mechanical testing. Finally, after determining the electrical conductivity as a function of electric field strength and temperature, electro-thermal simulations will be carried out in a

representative model joint (provided by NKT) by using COMSOL Multiphysics software.

1.4 Objectives

To achieve the above mentioned purpose, the following objectives has to be considered.

- Electrical testing such as conductivity (based on IEC 62631-3-1 standard), permittivity (based on IEC 62631-2-1 standard), dielectric loss (based on IEC 62631-2-1 standard) and AC breakdown tests (based on IEC 60243-1 standard) of various FGMs with different types of filler and varying their concentrations has to be done. As a part of initial screening, the conductivity measurement is first performed at 1 kV DC and if the result is within one order magnitude of magnitude of the reference values provided by NKT, then only go with the higher level of voltages in detailed screening to investigate the nonlinear conductivity. However, the permittivity and dielectric losses of materials are measured only at 1 kV AC. All the electrical tests except, AC breakdown tests have to be performed in different temperatures. Additionally, all the electrical testing is to be performed in 1 mm sample .

- The mechanical tests such as tensile, tear, elastic modulus and elongation at break (based on ISO 2285 standard) are performed with the sample with 2 mm thickness .

- The materials with nonlinear electrical conductivity and permittivity within the specified selection criteria are introduced in a representative HVDC joint model. The nonlinear electrical conductivity is introduced by fitting the measured data points to a mathematical model. Electrothermal simulations are carried out and the electric field distribution is investigated at various relevant locations in the cable joint such as the cable-joint interface.

2

Literature review

This chapter explains the important theories and gives an overview of past studies related to the topics covered in the master thesis.It starts with the electric fields and field grading mechanisms .

2.1 Electric field and stress control mechanisms

The electrical field at a given point is defined as the force experienced by the unit positive test charge placed at that point. That means , The electric field $\vec{E}$ is defined as the force $\vec{F}$ per unit charge $\vec{q}$, this can be expressed in the equation (2.1) .

$$\vec{E} = \frac{\vec{F}}{\vec{q}} \tag{2.1}$$

And electric field between two parallel plate electrodes can be defined by using below equation (2.2) , where V is the potential difference between plates, d is the distance between two parallel electrodes and $\hat{x}$ is the unit vector in the direction perpendicular to the plates.

$$\vec{E} = \frac{V}{d}\hat{x} \tag{2.2}$$

It is considered that the voltage V between two electrodes has to be insulated by placing a homogeneous insulating material with a breakdown strength "E_b" which is considered as the characteristic constant for each material. The needed distance of separation can be calculated using the equation (2.3) [3]

$$d_b = \frac{V}{E_b} \tag{2.3}$$

Even though, the electrodes are already defined in their size, the designer will has to care about entire field distribution between the electrodes and understand that in many cases, only a small portion of material is experiences the maximum field "$E_{\max}$". Thus "$E_{\max} = E_b$" provide the optimal solution for the insulation problems, which can be solved by studying the field analysis.

In multi-layer insulation systems, it's essential to understand how the field behaves across different materials with varying properties.

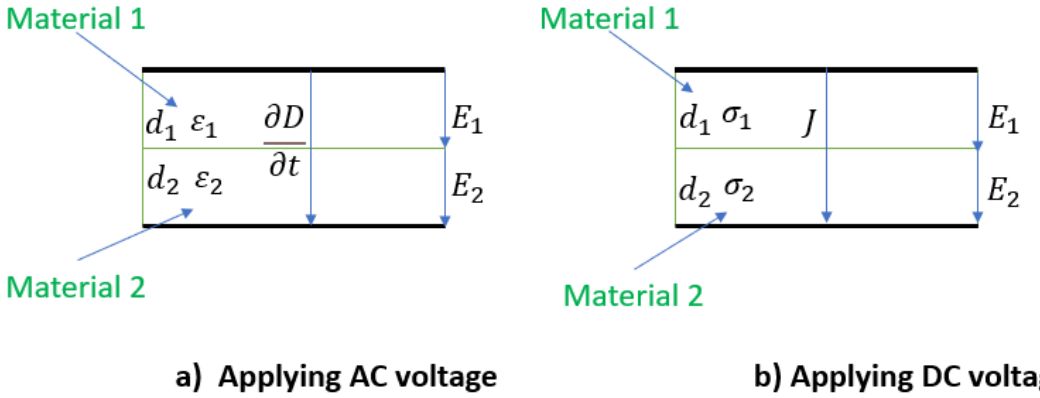

Figure 2.1: influence of AC and DC on different materials placed between two parallel plates

Figure 2.1 shows two materials with different thicknesses (d_1 and d_2) and different electrical material properties such as permittivity (ϵ) and conductivity (σ) placed between two parallel plates and applyind different voltages. The displacement current is denoted by $\frac{\partial D}{\partial t}$ and conduction current is denoted by "J".

For AC operation, displacement current dominates over conduction current "J" [2]. The total displacement current is the same through both materials and can be expressed by the equation below.

$$\frac{\partial D}{\partial t} = \epsilon_1 \frac{\partial E_1}{\partial t} = \epsilon_2 \frac{\partial E_2}{\partial t} \tag{2.4}$$

taking time interval on both side

$$D = \epsilon_1 E_1 = \epsilon_2 E_2 \tag{2.5}$$

, where "D" is the displacement density

$$\frac{E_1}{E_2} = \frac{\epsilon_2}{\epsilon_1} \tag{2.6}$$

if $\epsilon_1 \ll \epsilon_2$, then according to equation 2.4, more electrical stress will be transferred from material 2 to material 1.

For DC operation, only the conduction current exist, and the total conduction current through each material is same as shown by the equation below.

$$J = \sigma_1 E_1 = \sigma_2 E_2 \tag{2.7}$$

$$\frac{E_1}{E_2} = \frac{\sigma_2}{\sigma_1} \tag{2.8}$$

if $\sigma_1 \ll \sigma_2$, then based on equation 2.5, more electrical stress will be pushed from material 2 to material 1.
The electric field grading is referred as the technique used to reduce the local field enhancement of electrical devices to prevent breakdown or insulation failure, particularly in the high voltage applications. Essential field grading is important in insulation coordination. The design goals like cost, safety, and keeping electric fields and temperatures low can sometimes conflicts and need to be balanced. For instance, reducing the insulation thickness helps to reduce the material costs and lower temperature but higher electric fields, which might cause them breakdown, especially at important spots such as the interfaces or triple-points. Using the right field grading concepts can help to achieve a design that balances all these factors well [4]. Different field grading methods are described below.

1) Geometric field grading

In electrical systems, the electric field can be managed by introducing conductive surfaces that are connected to ground or high voltage. These surfaces, called electrodes, which will ensure that electric stress stays within safe limits. This method is called geometric field grading [5]. In cables, the shielding extends the ground potential outward, and the shape of conductive deflector gradually reducing the electric field strength from cable's surface outward. When cables are inserted into entry points, the deflector is placed inside a cone made of flexible material (grading cone) to further reduce electric field strength and enhance safety [2]. This can be used for all electrical stresses such as AC, DC and transient stresses like lightning and switching impulses.

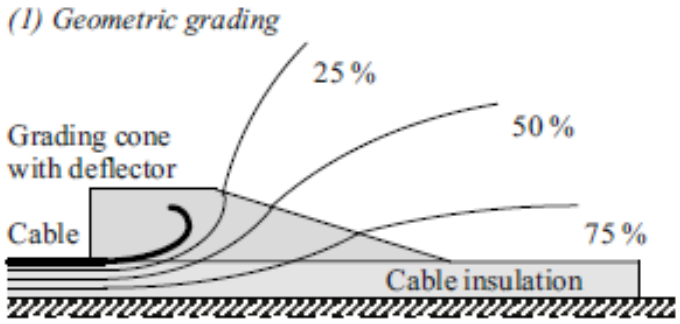

Figure 2.2: Geometric field grading [2]

2) Refractive field grading

To manage electric field distribution, a special tube made of a material with high permittivity can be added to the cable [2]. It is working based on the fact that under AC voltage, the field is pushed into the material or domain with lower permittivity. So a special material with higher permittivity compared to the cable insulation is used [2]. This can be used of AC and transient stresses like lightning and switching impulses and not DC.

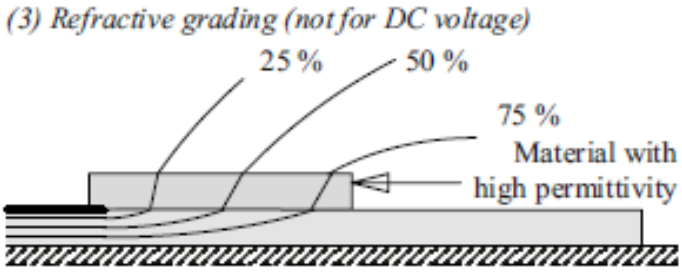

Figure 2.3: Refractive field grading [2]

3) Capacitive field grading

In the concept geometrical field grading, extra electrodes are added to the insulating material. But in capacitive field grading technique, these additional electrodes don't have a fixed electrode potential; instead, they adjust to a level that keeps the electric field between adjacent electrodes and nearby areas below the critical level. Capacitive field grading is used in high-voltage transformer bushings to manage electrical fields. To make the potential drop more even along the bushing, conductive foils are placed at regular intervals throughout its length. This helps to distribute the electrical potential more uniformly and improve the bushing's performance. It is mainly used for the AC or impulse electric field.

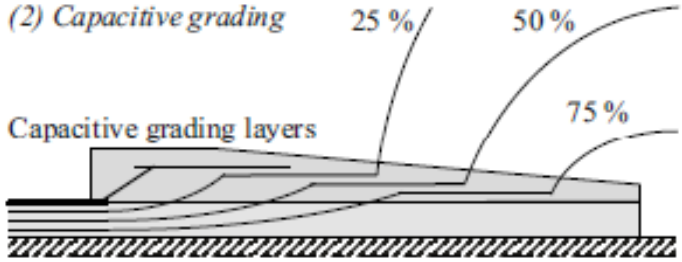

Figure 2.4: Capacitive field grading [2]

4) Resistive field grading

Resistive field grading is similar to refractive field grading but focuses more on conductivity. Just like in refractive field grading, the electric field lines bend in resistive field grading as well. It involves using a tube with higher conductivity to direct the electric field toward insulation with lower conductivity. However, this can be challenging because conductivity can change with temperature. For DC systems, there's an added issue: space charge can build up at the boundary between materials with different conductivity and permittivity [2]. This method works for both AC and DC and not for fast transient like lightning and switching impulses [5]. That's why nonlinear resistive field grading is used, which is explained in the next section.

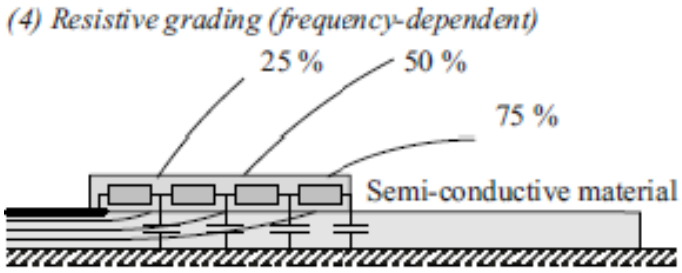

Figure 2.5: Resistive field grading [2]

5) Non-linear resistive field grading

Nonlinear field grading involves using materials that are highly insulating at low electric field strengths but become significantly more conductive as the electric field strength increases [2] . This behaviour helps to manage and reduce the electric field intensity at points where it is strongest [5]. In practical, the materials like ZnO (Zinc Oxide), SiC (Silicon Carbide), Feo (Iron Oxide) are embedded into polymer matrix and act as microvaristors. These microvaristors adjust their conductivity in response to electric field. At lower electric field, they act as insulators, while at higher strength, they conduct more electricity. This change in conductivity helps to redistribute the electric field. That means, the material with higher conductivity will push the field toward material with lower conductivity. More details about nonlinear resistive field grading techniques are covered in the upcoming chapters.

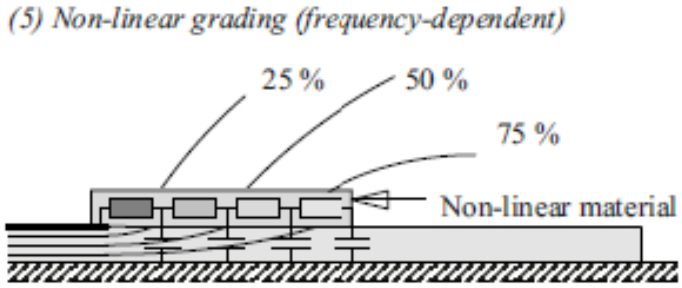

Figure 2.6: Non-linear field grading [2]

Additionally, the main concept of refractive and resistive field grading is that the field is pushed out the FGM into the adjacent materials. But these materials are usually high insulating materials such as XLPE, EPDM rubber, silicone rubber, epoxy etc. and these materials have a much higher breakdown strength compared to a highly filled FGM.

2.2 Filler particles

Filler particles are added to a polymer matrix to change it's properties such as permittivity, conductivity, etc. They can be evenly distributed or varied in concentration within material. Fillers are used to adjust permittivity or conductivity and also multiple fillers are also used to achieve specific properties [5].

Figure 2.7 [5] Depicts the representation of different filler types.Filler can be added homogeneously through the materials or with a spatial gradient of the concentration.

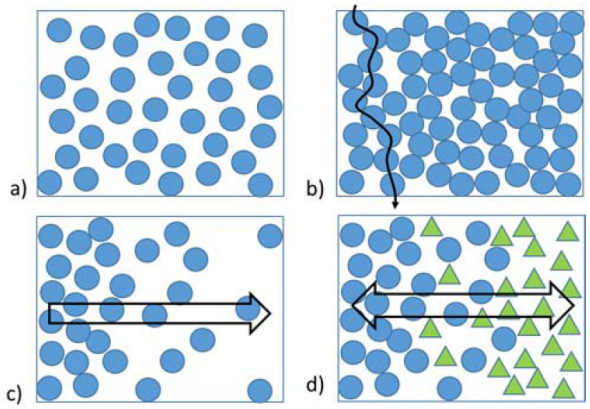

Figure 2.7: Representation of of different filler types: a) single filler homogeneously dispersed b) single filler homogeneously dispersed above the percolation limit (the arrow represents the one possible continuous path from one particle to the next) c) filler with spatial gradient d) system of two fillers with spatial gradient [5]

To enhance electrical conductivity, the filler concentration should exceed the percolation threshold. Conductive particles can be added to increase electrical conductivity of composite with higher concentration.

Permittivity is adjusted by altering the concentration of high permittivity fillers. Unlike conductivity, reaching the percolation limit is not required for permittivity changes. For permittivity , the fillers don't need to connect across whole material. They need to be there to help material to store more energy. While for conductivity, fillers must form a continuous path for current flow.

2.2.1 Conductive particles

Conductive or field grading applications require materials with low specific volume resistivity (less than 100 $\Omega \cdot$ cm) [5]. These materials are usually made from a polymer matrix combined with electrically conductive fillers. Carbon blacks are the most common fillers used. Conductive carbon blacks consist of primary particles that are typically between 1 and 100 nm in size [5]. These particles cluster together to from aggregates, which are smallest dispersible units. Aggregates are held together by van der waals forces and thus they are very strong. Thus, in practical use, carbon black is considered to be made up of these aggregates rather than individual primary particles. The aggregates come together and form agglomerates.
These aggregates are different in shapes and appeared in black color [5]. The different types of aggregates are showed in figure 2.8 [5]. Typically branched aggregates are easier to mix into polymer matrix and show better electrical conductivity.

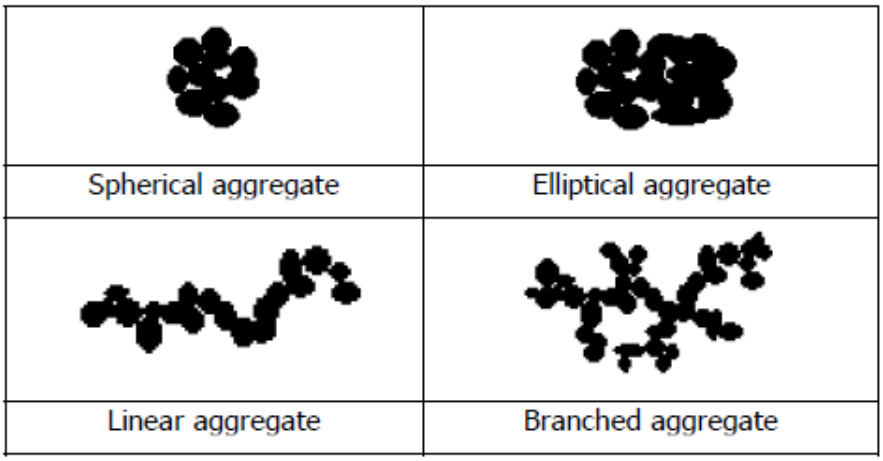

Figure 2.8: Classification of different types of carbon aggregates [5]

The electrical conductivity of polymer composites containing carbon black undergoes a significant alteration when the concentration of evenly dispersed carbon black reaches a critical point known as the percolation threshold. Prior to reaching this threshold and after this, the changes in the conductivity are minimal [5].

The percolation threshold level depends on various factors, including the conductivity of fillers, the type of polymer matrix, and the mixing process parameters [5].

Figure 2.9 [5] depicts the behaviour of the resistivity of a carbon black filled compound. It represent the resistivity of three polypropylene-carbon black compounds, each possessing different specific surface areas, in relation to the percentage of added carbon black [5].

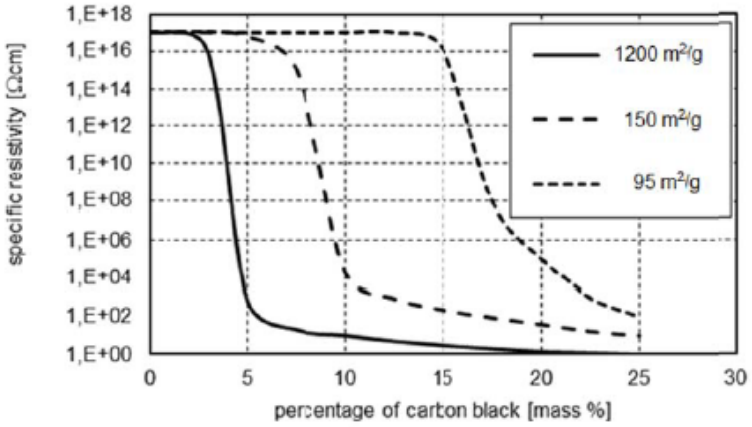

Figure 2.9: Resistivity behaviour of carbon black filled compound [5]

The electrical conductivity of carbon black filled materials is quite limited, because it relies on small contact areas between carbon black aggregates. Even though the conditions for applying the percolation theory may not be perfect for carbon black and typical polymers, it can still offer valuable insights into other effects, such as seen in heat- and cold-shrink field grading tubes filled with carbon black particles[5]. When these tubes are mechanically expanded, they have higher chances for forming a continuous path of electrical conduction because expansion reduces thickness in some directions,connecting separate clusters of carbon black particles to form larger conductive pathways. These effect is reversible, meaning conductivity decreases when the material returns to it's original state. Additionally, this process can cause changes in the electrical properties in different directions (anisotropic changes). However, it is important to note that mixing carbon black with polymers can significantly increase the viscosity of the mixture, which may limit it's practical use [5].

2.2.2 Nonlinear materials

Generally, Field grading materials are composite materials with one or more fillers particles being mixed with an insulation matrix. The materials showing nonlinear conductivity in dependence of electric field strength can be mainly divided into following groups.

1) Nonlinearity arises from particle to particle contact

Nonlinear conductivity in composite materials happens because of how particles, which can be either conductive or semiconductive, interact at their contact points. These particles are surrounded by a thin layer of oxide or another material, where surface charges build up and cause energy band bending, similar to what happens in Schottky barriers. This leads to nonlinear movement of electrons or holes through processes like hopping, tunneling, or thermal activation [27].
In materials like silicon carbide (SiC), carbon, and aluminum, thin oxide layers form naturally, making nonlinearity unavoidable. Semiconductive oxides are less reactive, so their nonlinearity is likely due to surface charges creating Schottky barriers at these contact points. When complex composites combine SiC with carbon black, different particle contacts are formed, which lowers the current needed to achieve conductivity. While thin polymer layers at these contacts might affect conductivity, they are not the main reason for nonlinearity, as it often appears even without the polymer [27].
These particle contacts are difficult to control and are very sensitive to factors like pressure, wear, and humidity. They can also degrade under electrical stress, making them vulnerable during manufacturing, stretching, or exposure to high temperatures and stress. Figure 2.10 [27] illustrate the internal structure of SiC based composites with current path, particles and polymer matrix.

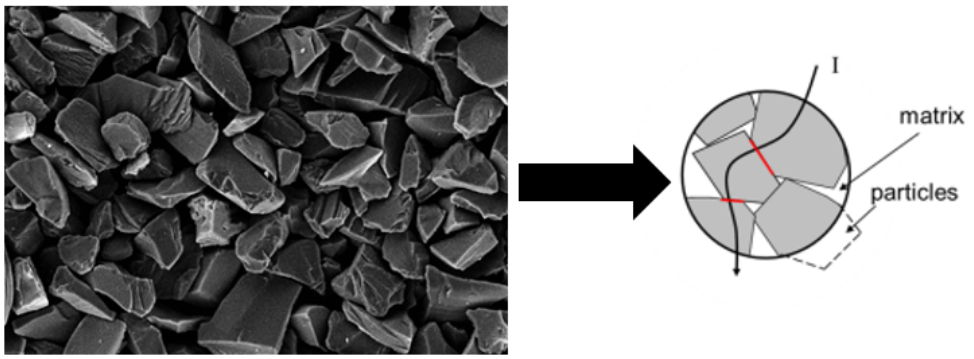

Figure 2.10: Illustration of internal structure of SiC based composite with the representation of path of current and particles and polymer matrix [27]

In figure 2.10, the interface of SiC particles are denoted by red colour. Potential barriers are formed between these interfaces which influences the nonlinear behaviour.
This type of nonlinear materials are based on a filler loading above the percolation threshold. This ensures a stable and predictable behaviour of the electrical conductivity with varying electric field. Below the percolation threshold, the fillers might not always be homogeneously dispersed which could result in very large batch to batch variations with regards to the electrical properties of the composite. But in case of such high filled composites the mechanical properties are very often weakened. However, when the filler particles having high filler ratio and different geometries, they can actually weaken the mechanical properties [27]. To improve these mechanical properties, some of the main filler particles have to be replaced by smaller conducting particles (secondary fillers), known as the bridging particles. These particles enhance the nonlinearity by reducing total filling ratio. In FGMs, common bridging particles carbon blacks, mica flakes, TiO2 etc[5]. Generally, carbon blacks are round in shape while mica flakes are irregular. Additionally, these bridging particles also have ability to handle the heat generated along the conduction path [27]. Generally, mica flakes are more convenient in dealing with the local heat when compared to carbon black [5]. Figure 2.11 shows how bridging particles are replaced by main fillers. The red circles marks where the bridging particles are at the interface to improve mechanical properties.

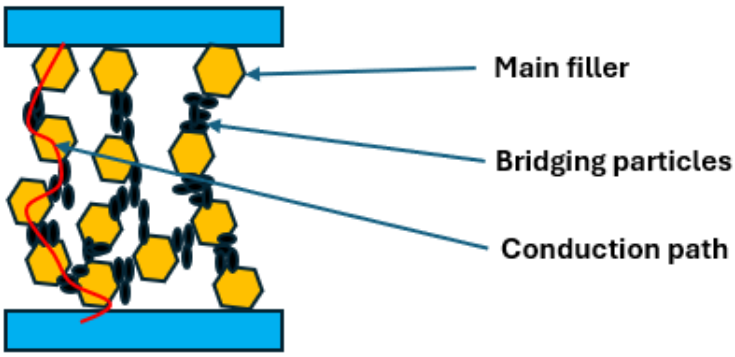

Figure 2.11: representation of bridging particles

2) Nonlinearity from the intrinsic property of the filler particles

In this type, the nonlinearity comes from the inherent properties of the interior particles themselves. These filler particles have low contact resistance. Microvaristors are an example of such filler particles. The nonlinearity of these particles is determined by the internal grain boundaries of the microvaristors. Conductive grains are seperated by electroactive grain boundaries, where electrostatic potential barriers form to control the current through the material [27]. The current flow increases exponentially up to a limit set by conductivity of the microvaristor grains. An example of microvaristor filler particle is ZnO (Zinc oxide). The electrical properties of ZnO depend largely on the number of grain boundaries, which means the size of the grains [27]. The electrical properties can be controlled by doping element, sintering temperature and time. Additionally, the mechanical properties can be improved by introducing the bridging particles at these internal grain boundaries. Figure 2.12 [27] shows the internal structure ZnO microvaristor with grains, matrix and particles, with the red line indicating the conduction path.

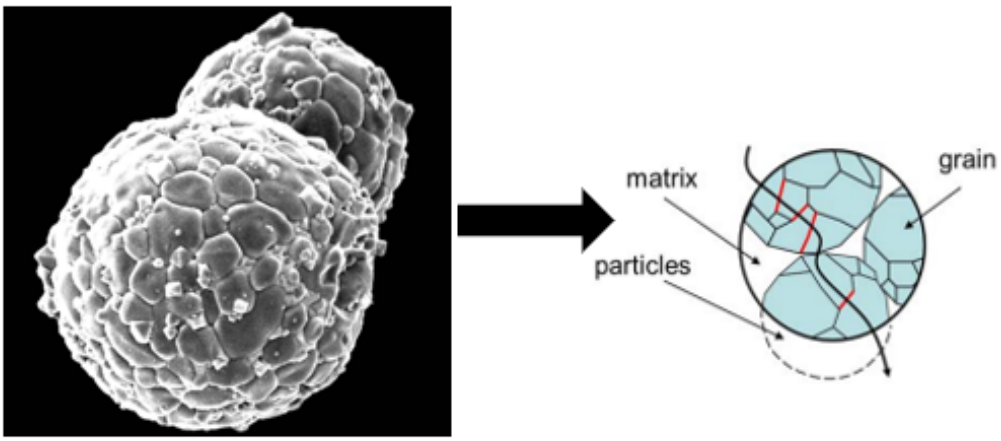

Figure 2.12: Illustration of internal structure of Zno based composite with the representation of path of current and particles and polymer matrix [27]

2.2.3 Physical properties of filler particles

As discussed in earlier, Polymeric composites with adding fillers such as SiC, carbon black, or blending various oxides such as BaTiO3, TiO2 or mica are used as the main FGMs for longer time. The physical properties of filler particles have greater significance for determining the electrical and mechanical properties of the field grading materials [6] . Generally, the polymer choices for the field grading materials in cable accessories are EPDMs and silicone rubbers, because rubber can be expanded and give a certain interface pressure on the cable which is very important to get a certain interfacial breakdown strength. These polymeric composite materials are reported to show their field grading functionality by their nonlinear resistive, refractive, or combined resistive and refractive response in the presence of locally generated electric stresses.

In a composite material which made up of a matrix and fillers , when the filler concentration exceeds percolation threshold, then continuous path can be formed within these fillers and allows the flow of electricity through the material, significantly affecting it's electrical properties. When the filler concentration is below the percolation threshold, the composite behaves as an insulator and the conduction path starts to develop above this percolation limits and exhibit nonlinear properties. The conduction paths can be straight or curved. Shortest conduction paths are with higher current density and they are with higher filler concentrations which leads to less switching field as well [6]. Figure 2.13 illustrates current density distribution after adding circular fillers into a polymer matrix with different filler sizes (**in part (a), the fillers are smaller, and in part (b), the fillers are larger**). The effects of contact resistance and other interface issues are not taken into account. Therefore, the shape of the conduction path is the only factor that affects the switching field.

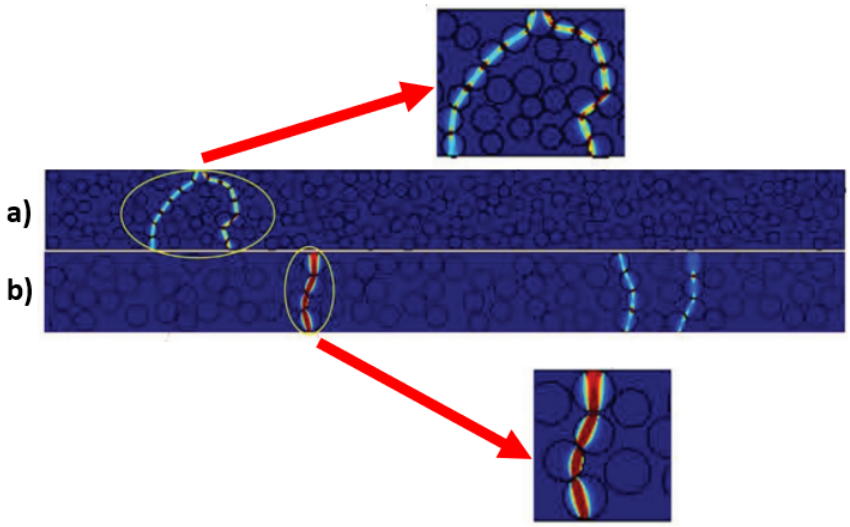

Figure 2.13: Current density distributions after incorporating circular fillers of varying sizes into the polymer matrix [6]

In Figure 2.13 (a), there are two conduction paths, whereas Figure 2.13 (b) shows three paths. This increase is due to the larger fillers creating more conduction pathways. The light blue to yellow regions represent lower current density, while the red areas indicate higher current density. Larger fillers result in higher current density, shorter conduction paths and lower switching field [6].
Nonlinear effects become significant when the electric field is very high. Spherical fillers, like carbon black, generally result in softer effective properties. However, non-spherical fillers, especially those with sharp edges, increase electric field amplitudes [8] . This "lightning rod effect" is more pronounced near the sharp corners of the fillers rather than on smooth, curved surfaces. Nonlinear properties of materials also become more prominent near the percolation threshold. In composites, the nonlinear susceptibilities change noticeably with the volume fraction of the constituents. This means that not only does the strength of the non-linearity generally increase, but the nature and type of nonlinear anisotropy also change when different materials are mixed [8] .

Figure 2.14 [6] illustrate the representation of contact interface between spherical (different in size) and irregular shaped fillers in both face and edge contact. In the case of irregular shaped fillers, the red portion indicates the fillers and white portion indicates the insulation matrix.

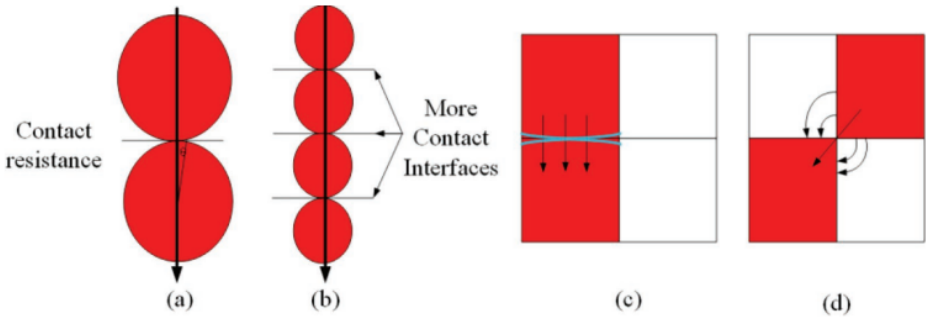

Figure 2.14: Representation of contact interface between spherical spheres (a) and (b) , irregularly shaped fillers in face contact (c), irregularly shaped fillers in edge contact (d) [6]

Equation 2.6 [6] represents the mathematical model to find contact resistance for spherical fillers (2.13 (a) and (b)).

$$R_c = \frac{1}{2}\rho_T \left[\frac{2}{3}\frac{E}{1-\nu^2}\right]^{1/3} F^{-1/3} \cdot r^{-1/3} \tag{2.9}$$

where:

- ρ_T is the Volumetric resistivity
- E is the Young's modulus
- ν is Poisson's ratio
- F is the Elastic force between fillers
- r is the Protrusion radius at contact point (depends on the filler diameter), which is difficult to determine in practice

From 2.14 (a) and (b), larger spherical fillers lead to lower contact resistance and a lower switching field. In contrast, smaller fillers have more contact points, which makes it harder for charge carriers to move. This results in higher contact resistance, lower conductivity, and a higher switching field [6].
The surface of irregularly shaped fillers is not perfectly flat. Face contact between these fillers can be considered as contact between two rounded fillers with a large radius of curvature, as shown in Figure 2.14 (c) [6]. Therefore, R_c for face contact can still be explained using Equation 2.6. And the arrows represent the conduction path. But contact interface for edge contact between irregularly shaped fillers are complicated. Two white squares represents the insulation matrix and two red squares represent the fillers. So the effective conductivity of irregular fillers in edge contact is represented by equation 2.7 [6] below.

$$\sigma_{\text{eff}} = \sqrt{\sigma_c \sigma_i} \tag{2.10}$$

where:

- σ_{eff} is the effective conductivity,
- σ_c is the Conductivity of the fillers,
- σ_i is the Conductivity of the insulation matrix.

Additionally, contact resistance for irregular shaped fillers with edge contact is much higher than that of spherical fillers. Thus higher switching fields are also expected.

The filler concentration, filler diameter and filler shape has greater influence on the electrical properties. Table 2.1 [6] depicts how filler properties effects the conduction path, contact resistance and switching field of nonlinear FGMs.

Filler properties	**Conduction path**	**Contact resistance**	**Switching field**
High filler concentration	Straight	Low	Low
Low filler concentration	Roundabout	High	High
High filler diameter	Straight	Low	Low
Low filler diameter	Roundabout	High	High
Round filler shape	-	Low	Low
Irregular filler shape	-	High	High

Table 2.1: Filler properties depend on the nonlinearities of FGMs [6]

2.3 Electrical conductivity

Electrical conductivity plays a crucial role in field grading techniques. FGM has higher conductivity than the surrounding insulations, such as cable or joint insulation. This difference in conductivity directs electric stresses away from the FGM and toward the surrounding insulation during normal operation. Conductivity measures how well a material can carry an electric current when voltage is applied. Conductivity is denoted by σ, and it's unit is Siemens per meter (S/m). Based on the level of conductivity, materials are classified into conductors, semiconductors and insulators. The conductivity range of different materials are depicted in figure 2.15 [2].

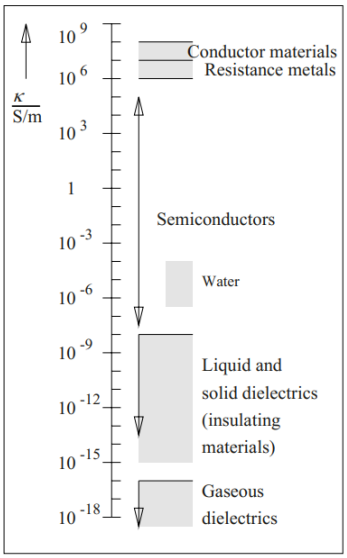

Figure 2.15: Conductivity range of various materials [2]

Simply, electrical conductivity can be described by equation 2.8 [28] below.

$$\sigma = \sum_{i=1}^{N_c} |q_i n_i \mu_i| \tag{2.11}$$

where:

- N_c is the number of charge carriers
- q_i is the charge of the charge carriers
- n_i is the volume density of charge carriers
- μ_i is the mobility of charge carriers

From the equation, it can be seen that the conductivity is primarily influenced by the volume density of charge carriers and their mobility. The charge of carriers in their magnitude is constant, so higher conductivity is achieved with a greater volume density of charge carriers [28]. However, the mere presence of charge carriers is not enough to increase conductivity. The carriers must be able to move between different energy states when a voltage is applied. If the charge carriers become trapped and cannot move, current cannot flow, leading to lower conductivity.

2.3.1 Measuring Conductivity with PDC setup

PDC (polarization and depolarization current) setup is used to measure the conductivity of material at different electric field strength. Figure 2.16 depicts the basic circuit of PDC test setup with shape of polarization and depolarization current.

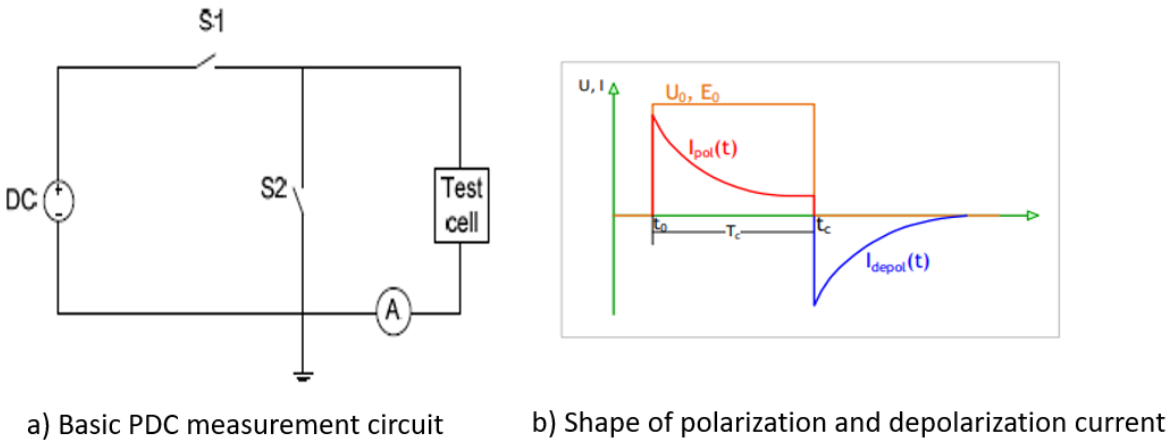

Figure 2.16: Basic circuit for PDC measurement with shape of polarization and depolarization current [30]

The test setup includes a high voltage source and measuring devices, with a computer controlling the switching and recording the current with a high-resistance electrometer. Switch S1 is closed and S2 is open during charging, and the current measured by the ammeter at this stage is called the polarization current. After charging, S1 is opened and S2 is closed to start the discharging process, with the ammeter measuring the depolarization current. Initially, when voltage is applied to the material, there's a sudden spike in current, known as the capacitive current. This current then decreases and stabilizes over time, which varies depending on the material. For more resistive materials, reaching a steady current can take several hours or even days. Afterward, the conductivity can be calculated using Equation 2.9.

$$\sigma = \frac{I_s\, d}{u \cdot A} \tag{2.12}$$

where:

- I_s is the steady state current
- d is the thickness of material
- u is the applied voltage
- A is the surface area of electrode

2.4 AC properties

2.4.1 Permittivity

As like conductivity, the permittivty has also greater significance in the field grading technique. The material with higher permittivty will pushes the field toward the material with lower permittivty. In the case of nonlinear resistive field grading technique, permittivty is more valid in the case of transient voltages like switching and lightning impulses. Permittivity describes how well a material can become polarized, or how its internal electric charges shift, when an electric field is applied.The higher the permittivity indicates more the material can be polarized and can store more electrical energy. Generally, there are different polarization mechanism which is depending on the frequency of the applied voltage.

In electronic polarization, an electric field causes the nucleus and the electron cloud to shift in opposite directions, creating tiny dipoles. This effect happens in all materials but is usually small compared to other types of polarization. However, it happens very quickly, so the polarization is almost unaffected by changes in the frequency of the electric field [5].

Atomic polarization occurs in substances with different non-ionic atoms. The negative charges move towards the more electronegative atoms, creating a permanent dipole. In this polarization,the nuclei within the molecule shift relative to each other [5].

Ionic polarization is like atomic polarization but involves the movement of ions species when an electric field is applied.

In orientation polarization, permanent dipoles align themselves with an applied electric field. This type of polarization is most effective in liquids and gases. For example, water has a high dipole moment and shows strong orientation polarization.

Each type of polarization in a material is effective only within a certain frequency range and is defined by relaxation frequency. When the frequency goes beyond this frequency range, depolarization can no longer contributes to the permittivity of the material.

Figure 2.17 [5] represents the dielectric permittivity (with real and imaginary part) spectrum for unitary materials over wide range of frequencies.

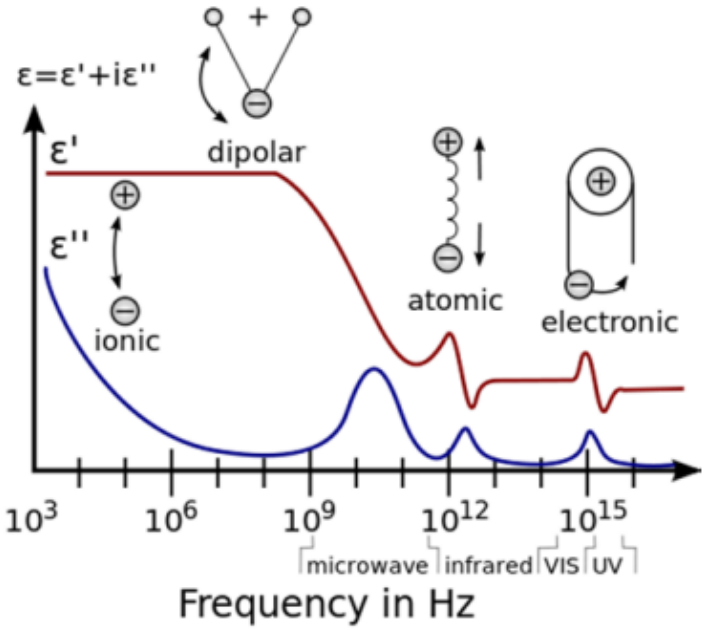

Figure 2.17: Dielectric spectrum for unitary materials [5]

The permittivity of a material placed between two electrodes (one with high potential and the other grounded) can be found using equation 2.13 [2].

$$\varepsilon_r = \frac{C \cdot d}{\varepsilon_0 \cdot A} \tag{2.13}$$

where:

- C is the measured capacitance of the material placed between the electrodes,
- d is thickness of the material,
- ε_0 is the vacuum permittivity ($\approx 8.854 \times 10^{-12}\,\mathrm{F/m}$),
- A is the area of the electrodes.

2.4.2 Dielectric loss (tangent delta)

In a Field Grading Material (FGM), measuring dielectric loss is crucial to understanding its efficiency. For an ideal FGM, dielectric losses should be kept to a minimum. Dielectric loss refers to the energy lost as heat in a dielectric material when it is exposed to an alternating electric field. The dielectric losses should me minimum for an ideal FGM. In a perfect capacitor, the voltage "V" and current "I" are phase shifted by 90 degrees (as shown in Figure 2.19(a)), meaning the current is purely capacitive [31]. However, if there are impurities in the dielectric material, it reduces the insulating resistance, causing some of the current to be resistive [31]. As a result, the insulation no longer acts as a perfect capacitor, and the voltage and current will not be 90 degrees phase shifted anymore, as shown in Figure 2.19(b) . The change in the phase shift indicates the tangent delta, which reflects the level of aging or deterioration in the insulation.

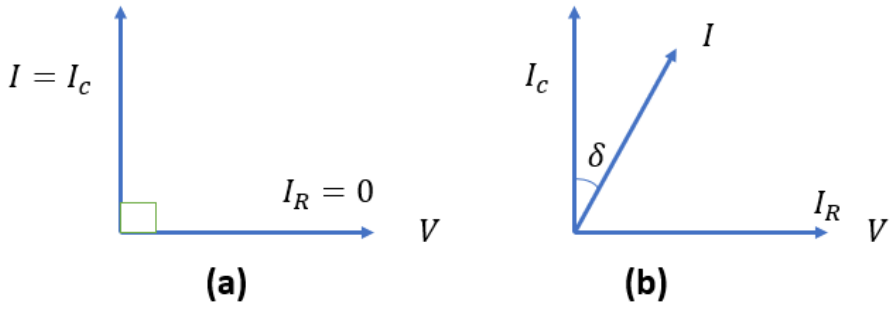

Figure 2.18: V and I representation in a capacitor without and with dielectric losses

Tangent delta of dielctric placed between two electrodes (high potential electrode and ground potential electrode) can be measured by using equation 2.11 [2] below

$$\tan \delta = \frac{1}{\omega C R} \tag{2.14}$$

where:

- ω is the angular frequency of the applied alternating current (AC) voltage ($\omega = 2\pi f$, where f is the frequency),
- C is the capacitance of the dielectric material between the electrodes,
- R is the resistance of the dielectric material.

5

2.5 Electrical design of nonlinear FGM

Linear field grading is more beneficial for normal operation. This means, the conductivity of FGM is greater than that of surrounding insulation material which pushes electrical stresses toward surrounding insulation material [7]. The breakdown strength of insulation material is much higher than that of FGMs. To prevent overheating, the conductivity must not bee to high at operating electric field strength.
Nonlinear FGMs have a conductivity that changes based on the electric field applied to them. When the electric field is low, their conductivity is also low, but as the field strength increases, their conductivity increases. This ability to control conductivity with the electric field is useful in regular operations as well as in transient situations like lightning and switching impulses. Additionally, nonlinear FGMs help distribute electric stresses more evenly in irregular shapes. This results in a more uniform stress distribution, achieved through refractive field grading. For example, if the stress is high at a specific point, such as near an electrode, the FGM in that area becomes more conductive and spreads the stress to the surrounding material.

Figure 2.20 [7] below represent the (nonlinear conductivity versus electric fields) κ-E characteristics of nonlinear field grading materials.

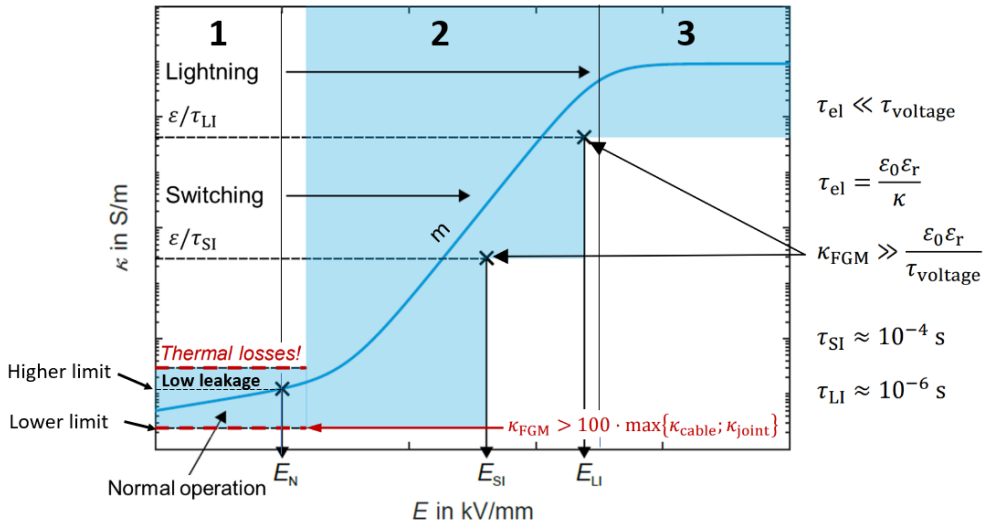

Figure 2.19: κ-E characteristics of nonlinear field grading material [7].

Region 1 represents the lower conductivity region. Many materials show linear κ-E characteristics for low field strength. The lower limit of base conductivity of this region is determined by the equation below, where κ_{near} represents the conductivity values of the cable insulation or joint insulation [5].

$$\kappa_0 \geq 100 \cdot \max(\kappa_{near})$$

In region 1, if the conductivity goes above the higher limits, it will lead to thermal losses and can cause thermal runaway. The higher limits of the region 1 is decided by switching field.
During normal DC operation, the field grading is happening due to the combination of resistive and geometrical field grading. This causes the field grading material (FGM) with higher conductivity to push the electric stress toward the cable or joint insulation.

Region 2 represents the location at which the material shows strong non linearity. Electric field strength above which nonlinear material exhibit sudden increase in electrical conductivity described as the switching field (E_N). The nonlinear increase of the conductivity levels above the switching field is required to achieve resistive field control during transient voltages. These required conductivity levels are set based on the relation between electrical time constant of the FGM ($\tau_e l$) and time constant of applied voltages (τ_{Voltage}) [20]. To achieve resistive field control during transient cases, the time constant of voltage must be much greater than electrical time constant of the FGM ($\tau_e l \ll \tau_{\text{Voltage}}$) as shown in figure 2.21. Therefore, $k_{\text{FGM}} \gg \frac{\epsilon_0 \epsilon_r}{\tau_{\text{voltage}}}$. The time constant of lightning impulse τ_{LI} and switching impulse τ_{SI} are approximated in to 10^{-6} and 10^{-4} respectively. Additionally, in region 2, resistive field grading technique with refractive and geometrical field grading takes place during transient cases. Thus the permittivity is also important. The FGM with higher permittivity will pushes the electric stress toward the cable insulation or joint insulation.

Region 3 represents the saturation zone. Here, nonlinear FGMs show that their conductivity stops increasing and levels off.

2.6 Breakdown in solids

The ability to handle high voltages without breaking down is crucial for FGMs. This ensures even distribution of electric fields and preventing them from exceeding from material's limit. Breakdown mechanisms in solids are the processes when a solid dielectric undergoes electrical failures due to high voltage stresses, leading the formation of conductive path through the material. These breakdown mechanisms are complex and can be influenced by various factors such as nature of electric field, temperature, humidity, etc. The different breakdown mechanisms are explained in next sub chapters.

2.6.1 Intrinsic breakdown

Intrinsic breakdown depend upon the presence of free electron to gain enough energy to ionize the atoms in the lattice structure. This creates free electrons and holes, leading to the formation avalanche charge carriers and cause breakdown. Mainly there are two types of intrinsic breakdowns. That are electronic breakdown and avalanche breakdown [29].

Electronic breakdown occur in the order of 10^{-8} seconds. It starts with a high initial density of free electrons. When an electric field is applied, the electrons gain energy and jump from the valence band to the conduction band. As this process continues, more electrons move to the conduction band, leading to a breakdown [29]..

Avalanche breakdown is similar to gas breakdown through cumulative ionization. In this process, an electron within the dielectric moves from the cathode to the anode, gaining energy from the electric field and losing it during collisions. When the energy gained by the electron exceeds the lattice ionization potential, it liberates an additional electron upon collision. This chain reaction continues, forming an electron avalanche. Breakdown occurs when this avalanche surpasses a critical level [29]..

2.6.2 Electromechanical breakdown

When solid dielectrics are exposed to high electric fields, it can create mechanical stress within the material. This stress can lead to cracking or even breakdown of the dielectric material.

2.6.3 Thermal breakdown

It is the phenomenon in which the dielectric material fails due to the excessive build up of heat, often as result of of dielectric losses or electric stresses. The increased temperature cause increase in the conductivity and further heating and gradually cause breakdown.

2.6.4 Partial discharge

When the local electric stress in a solid dielectric exceeds a critical level, it can cause localized discharges at defects, voids, or surfaces within the dielectric. These discharges, called partial discharges, can gradually lead to the breakdown of the material.

2.6.5 Water treeing

When solid dielectrics come into contact with salt water or electrolytes and are subjected to lower electric fields (greater than 2 kV/mm), these substances can enter small voids within the material. This can create tree-like structures inside the dielectric. Over time, these structures weaken the material's insulating properties and can eventually cause it to fail. This process occurs specifically with AC electric fields.

2.6.6 Electrical treeing

A very strong divergent electric field (greater than 100 kV/mm) can create tiny voids in dielectric materials. These voids lead to partial discharges that form tube-like structures, advances damage to the insulation. Carbon deposits on the walls of these structures increase the electric field at the tips of the trees. This process is irreversible and will eventually cause the insulation to completely fail. This damage can happen with both AC and DC electric fields.

2.7 Mechanical properties

High voltage cable joints are made from polymers like silicone rubber and EPDM. Mechanical properties are crucial in these joints because these rubbers can be expand and apply pressure on the cable, which is essential for achieving strong interfacial breakdown resistance. Good mechanical strength ensures the joint won't fail during installation, use, or due to environmental changes. This thesis will focus on measuring four key mechanical properties, which are explained briefly.

2.7.1 Elastic modulus

Defined as the measure of material´s stiffness or rigidity. It describes about the ratio between the stress (force per unit length) and strain (deformation) in a material in linear elastic region of stress-strain curve. Higher elastic modulus means, the material can deforms less under applied stress. However, lower elastic modulus indicates a more flexible material. Elastic modulus can be explained by equation 2.12

$$E = \frac{\sigma}{\varepsilon} \tag{2.15}$$

- E : Elastic modulus
- σ :Stress
- ε :Strain

2.7.2 Tensile strength

Maximum amount of stretching stress a material can withstand without failure. It is determined by subjecting a material sample to controlled tension until it breaks. Therefore, high tensile strength indicates a materials ability to withstand high stress before breaking.

2.7.3 Elongation at break

It is defined as the amount of material can stretch or elongate before breaking, expressed in percentage of the original length. The elongation at break can be calculated by using equation 2.13

$$E_L = \left(\frac{X_F - X_0}{X_0}\right) \cdot 100\% \tag{2.16}$$

- E_L is the elongation at break in percentage,
- X_F is the final length at the breaking point,
- X_0 is the original length before deformation.

2.7.4 Tear strength

Defined as the resistance of material against tearing. It measures the force required to propagate a tear once it has been initiated. Higher tear strength means, the material is highly resistant to tear

2.8 Materials to be tested

Three materials with varying concentrations of secondary fillers will undergo electrical and mechanical tests. Model data from NKT is used as a references, which the different compounds will be compared to on a relative scale, therefore results are shown in normalized form. Table 2.2 shows the materials and their types of secondary fillers. Samples with different filler levels should be within a set of selection criteria.

Type of materials	Polymer matrix	Type of filler
Type A	EPDM	Carbon black fillers with smaller particles
Type B	EPDM	Mica flakes fillers with larger particles
Type C	EPDM	Carbon black fillers with medium particles

Table 2.2: Materials used for testing

Definition of particle size
smaller particles : less than $0.5\mu m$
Medium particles : less than $3\mu m$
larger particles : greater than $5\mu m$

For this thesis and for the simulations, it has been assumed that materials are EPDM based. Additionally, it has to be clear that, the simulation are not doing on a "real" joint, but a model of a possible HVDC joint.

2.9 Overview of overall testing procedure

The overall testing process is illustrated in Figure 2.20. Testing is divided into initial and detailed screening, with detailed screening being more time-consuming and taking approximately two days to complete. The initial screening includes testing electrical and mechanical properties. Electrical tests are conducted at 1 kV at both 25°C (room temperature) and 90°C. Detailed screening involves measuring nonlinear conductivities at four confidential voltage levels at 25°C, 70°C and AC breakdown voltage measurement of selected candidates based on candidates selection criteria. Additionally, the initial screening requires measuring four mechanical properties: elastic modulus, elongation at break, tensile strength, and tear strength. Detailed screening is only performed if the conductivity measured in the initial screening is up to 10 times higher than the reference value. The reference values are given by NKT.

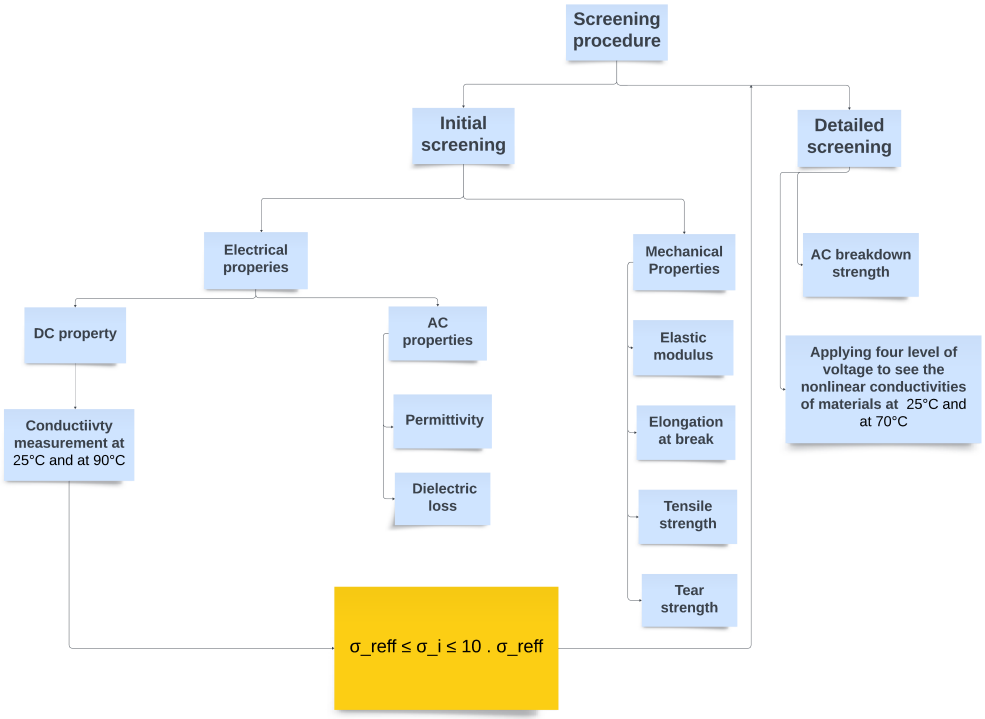

Figure 2.20: Overview of overall testing procedure

Good candidates selection criteria based on the material properties are described in the table 2.3

Material Properties	Selection criteria
Conductivity	$\sigma_{\text{reff}} \leq \sigma_i \leq 10 \cdot \sigma_{\text{reff}}$
Permittivity	$\geq$ reff
Dielectric losses	$\leq$ reff
All mechanical properties	$\geq$ reff

Table 2.3: Good candidates selection criteria for materials

3

Methods

This chapter describes the methods used for accomplishing the thesis objectives. It mainly describes about the experimental setups and procedure used for the electrical characterisation of the field grading materials. It starts with the equipment used for the electrical characterization of the materials for the initial screening purpose.

3.1 Initial screening

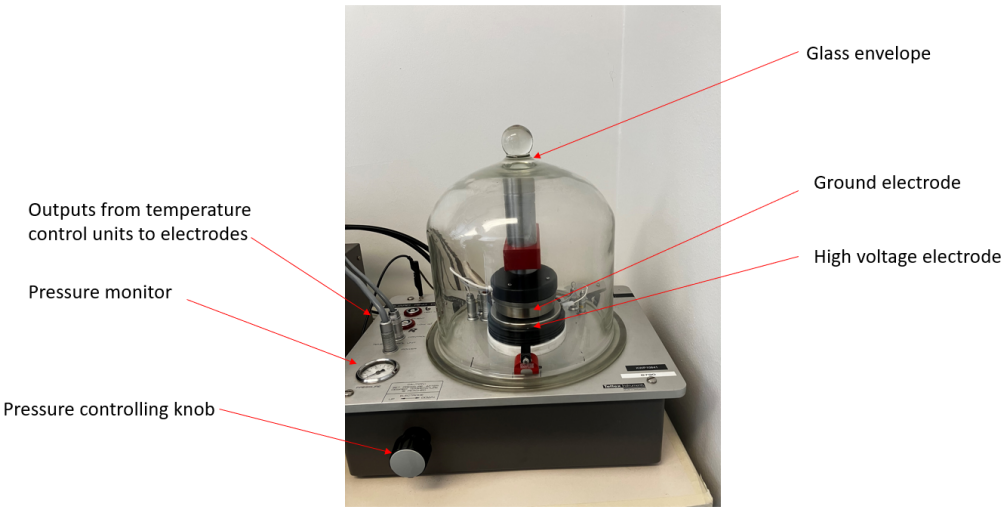

Figure 3.1: Electrical properties measuring device for screening

Figure 3.1 represents the overview electrical properties measuring device for the initial screening purpose. From the figure it can be seen that the high voltage electrode is fixed at the bottom and ground electrode is placed at the top. Temperature control unit is connected to both of these electrodes (see figure 3.2). It is possible to adjust the temperature of the test cell between room temperature and 300°C, therefore it can be adjusted according to the testing procedure Pressure can be adjusted by using the pressure controlling knob and and it can be monitored by the pressure monitor. Additionally, there is an glass envelop used to avoid the external distractions during testing process.

The initial electrical screening will be carried out at 1 kV, where both permittivity and dielectric losses will be measured at 1 kV AC. These properties can be assessed by connecting a Schering bridge (see figure 3.3) to the test cell. Similarly, electric conductivity will be measured under a 1 kV DC voltage by connecting a high resistance meter (see figure 3.4) to the test cell.

Figure 3.2: Temperature control unit

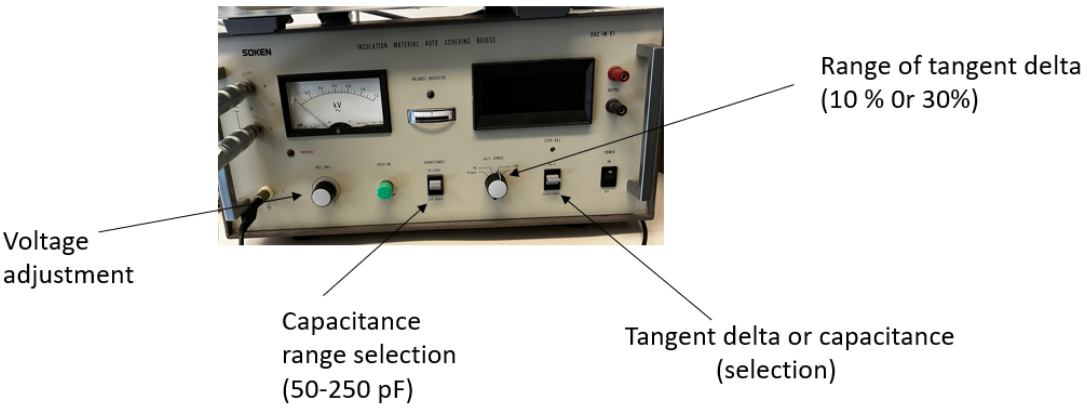

Figure 3.3: schering bridge

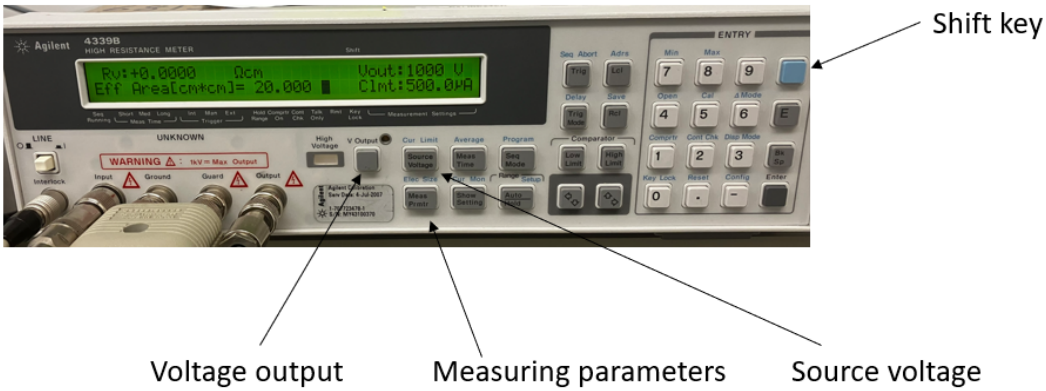

Figure 3.4: high voltage resistance meter

The freshly prepared sample should be kept in an oven at 80°C for 24 hours to allow degassing. After removing it, let the sample cool for one hour before conducting any electrical tests; otherwise, the residual heat could impact the measurements. According to IEC 62631, measure the thickness at five points where the electric field will be applied, then calculate the average thickness. Figure 3.5 indicates where to measure the thickness on each plaque sample.

Figure 3.5: Thickness measuring points

3.1.1 Procedure of initial electrical screening

The rested or discharged sample (samples should be discharged for at least 2 hours) should be placed between the high-voltage electrode and ground electrode at the exact black-marked position shown in Figure 3.6. After placing the sample, the glass cap should be secured on the test cell. Additionally, the pressure in the test cell should be adjusted to 2 N/cm^2 using the pressure control knob.

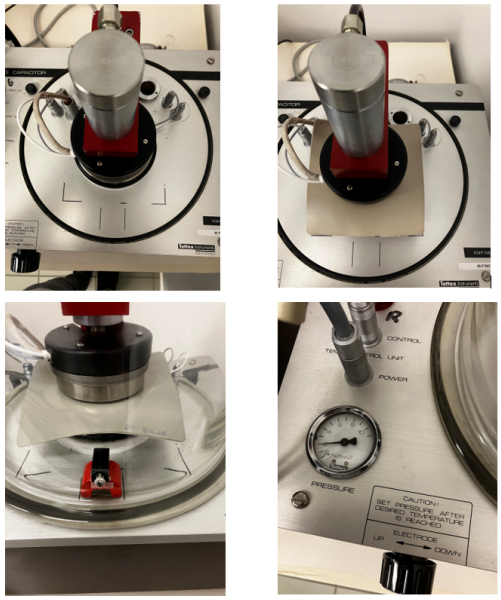

Figure 3.6: illustration of placing sample inside test cell

The initial screening process involves (see figure 2.20) testing the electrical properties at two temperatures: first at room temperature (25°C) and then at 90°C, with a voltage of 1 kV applied for 1 hour. If the materials meet the selection criteria (see table 2.3), more detailed screening will be conducted, including AC breakdown test and non-linearity conductivity tests at four different voltage levels and various temperatures.
Once the desired temperature is selected on the temperature control units, it is mandatory to wait for 10 minutes to reach temperature inside the sample.
Typically, it is necessary to perform both electrical conductivity measurements and AC measurements on the same sample. In such a cases, the AC test has to be performed first, then followed by a 5 minute interval before electric conductivity measurement.

In order to measure the AC properties , the test cell has to be connected with schering bridge and temperature control unit. After reaching the desired temperature on the sample , turn ON the schering bridge and the voltage can be applied after turning the green knob ON and then adjust the voltage control knob to apply voltage of 1 kv AC (see figure 3.3). To measure the tangent delta, initially set the range of tangent delta of 30 % and, then reduce the range for more precise measurements. Starting with a smaller range can result inaccurate reading because the device will display incorrect values if the tangent delta exceeds the desired range.

To measure the permittivity, the capacitance of the sample should be measured, typically the capacitance range should be set a range between 50-250 pF for the rubber materials. To measure the capacitance, change the selection switch from tangent delta measurement to the capacitance measurement (ref figure 3.3), then measure the corresponding capacitance and then calculate the permittivity according to the equation (3.1) which is provided in the operation manual.

$$\epsilon = C_m \times d \times 0.5647 \tag{3.1}$$

Where:

- ϵ is the permittivity of the material.
- C_m is the measured capacitance.
- d is the thickness of the sample in cm.

In order to measure the electrical conductivity, the test cell has to be connected with the high- resistance meter device. The next step is to set the thickness of the sample.The thickness can be measured by using digital thickness measuring device

Both of these parameters can be set by using the measuring parameters tab in the high voltage resistance meter (see figure 3.4). And then set the output voltage as 1 kV DC using source voltage tab and then apply the voltage to the material by pressing voltage output and then measure the conductivity.

3.2 Detailed screening

The non-linear conductivity of the field grading materials can be measured by using PDC measurement setup as shown in figure 3.7.

Figure 3.7: Overview of PDC measuring setup

The setup includes a DC voltage source, a climate chamber, a water deionizer, an electrometer, and a computer. The test cell features three electrodes: a high voltage (HV) electrode, a ground electrode, and a guard electrode. The DC voltage source is connected to the HV electrode inside the climate chamber, with the sample placed between the HV and ground electrodes. Conductivity is measured through the material, while the guard electrode detects surface current that could affect the measurement. Connecting the guard ring to the ground eliminates surface current, allowing measurement of only the current through the material. The ground electrode is linked to the electrometer to track the material's conductivity over time. The water deionizer ensures a stable environment by maintaining controlled moisture levels within the climate chamber, preventing fluctuations and noise. Additionally, a specialized computer program controls the experiments.

Figure 3.8 provides a close-up view inside the climate chamber. It shows FGM material positioned between high voltage and ground electrodes. A low BNC cable connected to the electrometer measures conductivity continuously. A dummy test cell is positioned behind the main test cell, where a temperature sensor is placed within a rubber sample., which helps track when the test sample reaches the desired temperature for more precise monitoring.

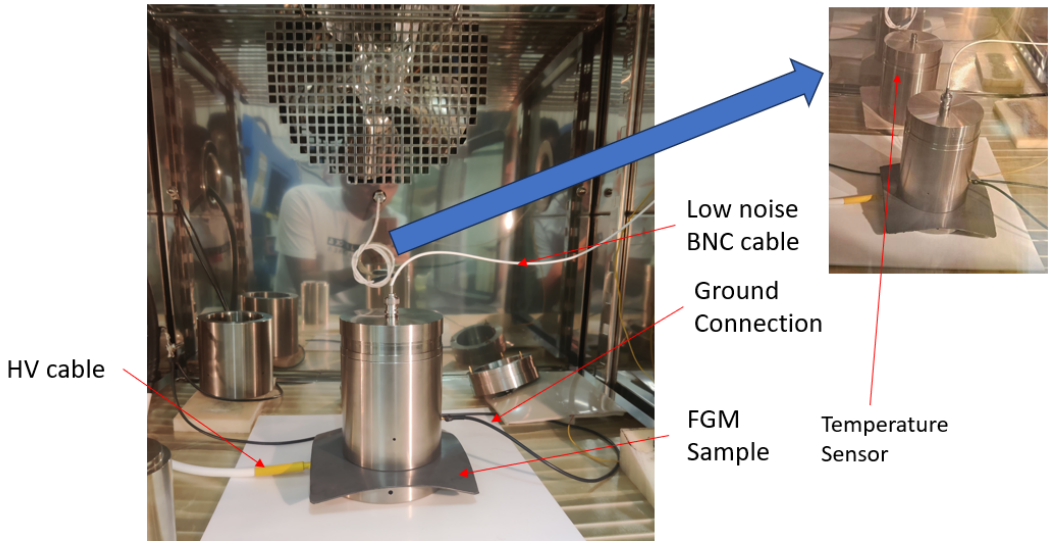

Figure 3.8: Detailed view inside climate chamber

3.2.1 Procedure of nonlinear conductivity measurement

The main goal of this test is to measure the conductivity of field grading materials at four different electric field levels. All subsequent results will be presented as normalized values. Additionally, the test is conducted at various temperatures to analyze how conductivity behaves nonlinearly compared to reference material.

The nonlinear conductivities are measured at four undisclosed electric field levels (with normalized electric fields provided in the "Results and Discussion"), as well as at room temperature (25°C) and 70°C. After each voltage level measurement, the sample must be discharged for one hour.

Figure 3.9 displays the programming window for PDC measurement. Nonlinear conductivity is first measured at 25°C for each voltage level. The figure shows that the electric field begins to be applied after a 2 hour of waiting period, because it takes 2 hours to reach temperature inside sample.

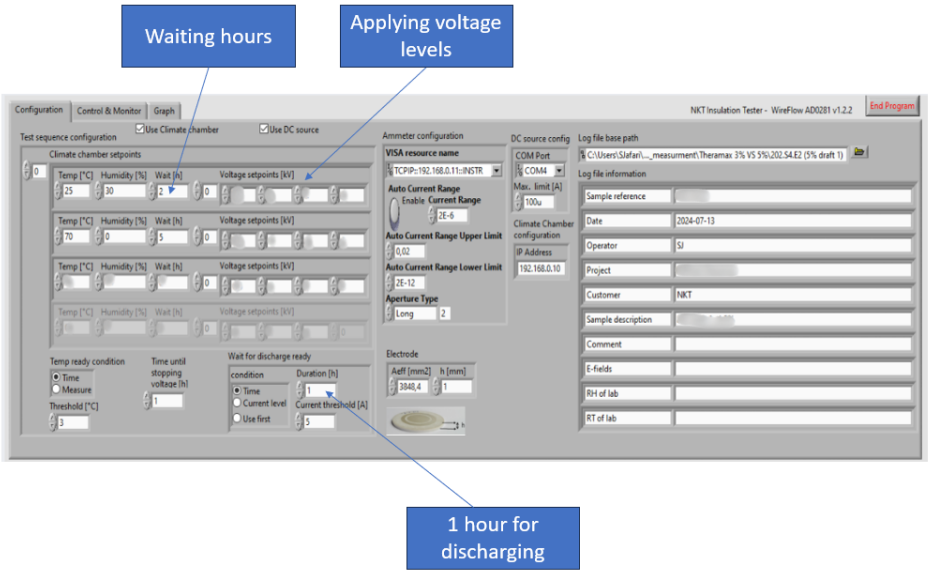

Figure 3.9: Programming window for conductivity measurement

Following the same procedure for measuring conductivity at 70°C. It takes about 5 hours for the sample to reach this temperature. The sample's temperature is raised by heating the climate chamber, unlike the initial testing where separate temperature control units were directly added to the electrodes. Once the temperature is reached, start the program. Set the discharging time after applying each electric field to 1 hour.

3.2.2 AC breakdown voltage measuring test setup

Figure 3.10 illustrates the experimental setup for the AC breakdown test. The setup generally includes a high-voltage power supply, a test cell with electrodes, and measurement instruments. The high-voltage power supply applies alternating current (AC) to the test cell, where the sample is placed between the electrodes. Additionally, this breakdown test is carried out in castor oil.

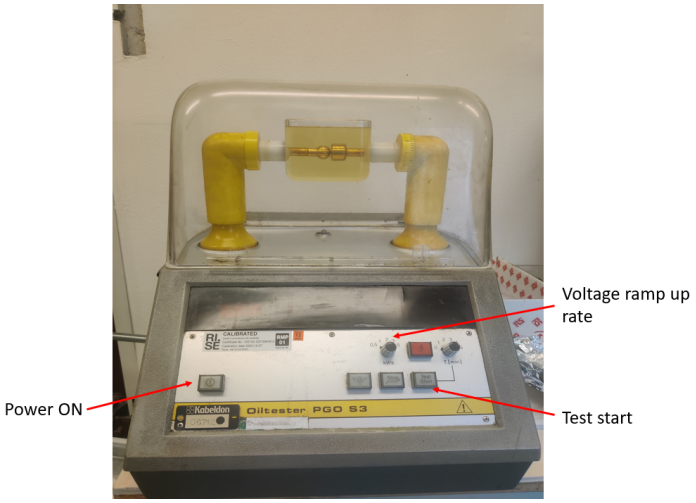

Figure 3.10: AC breakdown experimental setup

3.2.3 Experimental procedure

A typical plaque sample is 150 mm × 150 mm and having 1 mm thickness. Five round test objects are stamped from one plaque sample for AC break down testing. After cleaning the test object with non particle tissue and the ethanol, the thickness of each test object has to be measured. For the field grading materials the voltage ramp up rate should be set it as $0.5\,kV/s$. Before performing each test, It is essential to ensure that the area between electrodes should be clean and free of any particles or air bubbles. For each sample, five breakdown measurements are required, and the median Breakdown values are reported. If any of test result deviates more than 15 % from the median, again five additional test has to be conducted. Then the breakdown voltage should be determined from the median of the 10 results. The test is performed based on IEC60243-1. The oil in the breakdown test should be changed after 25 breakdown tests. And during this 25 breakdown test, only one type of the material should be tested, and new oil should be used when we change the material. Figure 3.11 represents the detailed view of the ac breakdown test setup. Put the sample between two electrodes, turn on the device, and start the test. The device will increase the voltage gradually and measure the point at which the sample breaks down. After breakdown sample is taken out from oil to to visually inspect the breakdown point.

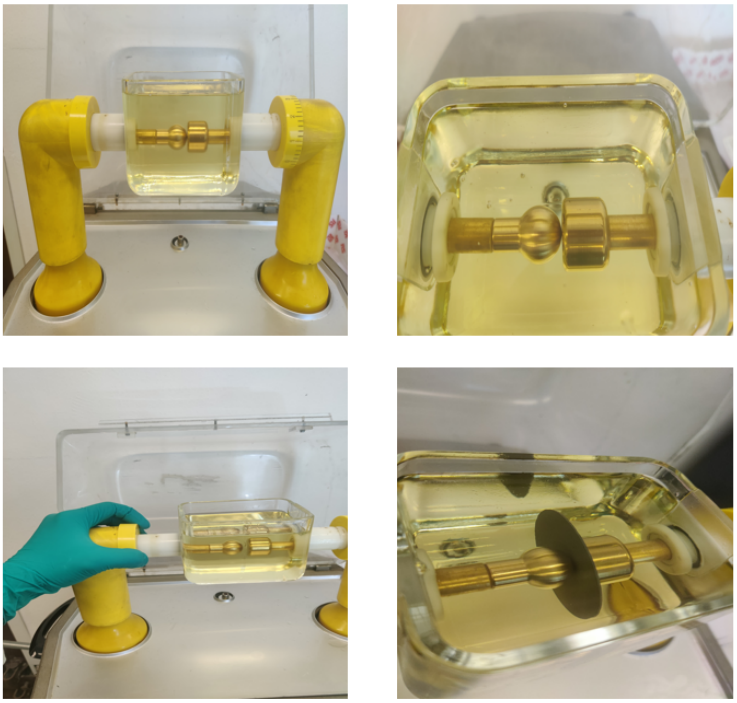

Figure 3.11: Detailed view of ac breakdown test setup

3.3 Mechanical properties

The mechanical properties, including E-modulus, tensile strength, elongation at break, and tear strength, are tested using 2 mm samples. These samples are cut into various shapes refer to the standard shape required for each mechanical tests. For example, figure 3.12 shows the shapes used for E-modulus, tensile strength, and elongation at break tests. Four samples are used for each test, and the average value is recorded. Tear strength tests uses another shape as shown in figure 3.13 and are conducted with a specific program. Detailed overview for testing tensile and tear strength are illustrated in figures 3.14 and 3.15, respectively.

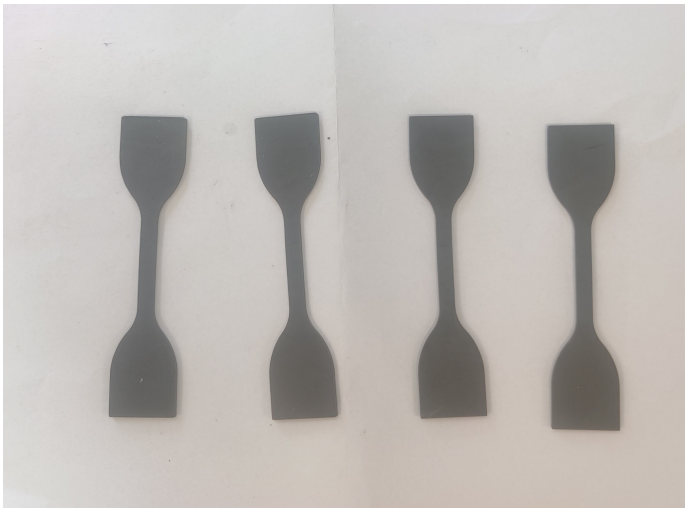

Figure 3.12: shape of sample used for tensile strength

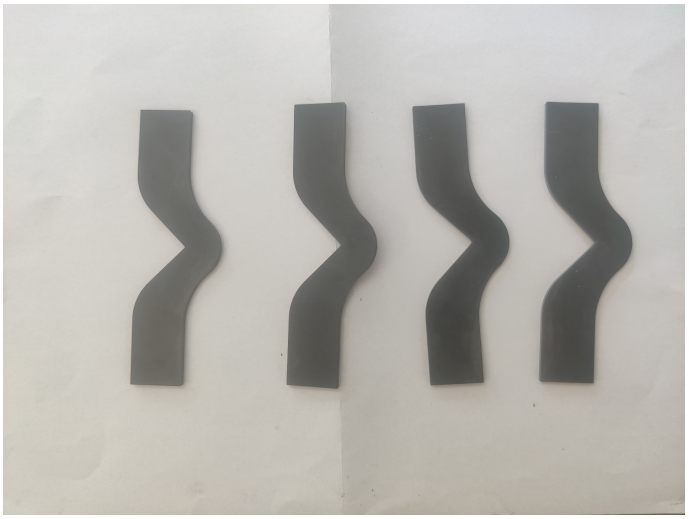

Figure 3.13: shape of sample used for tear strength

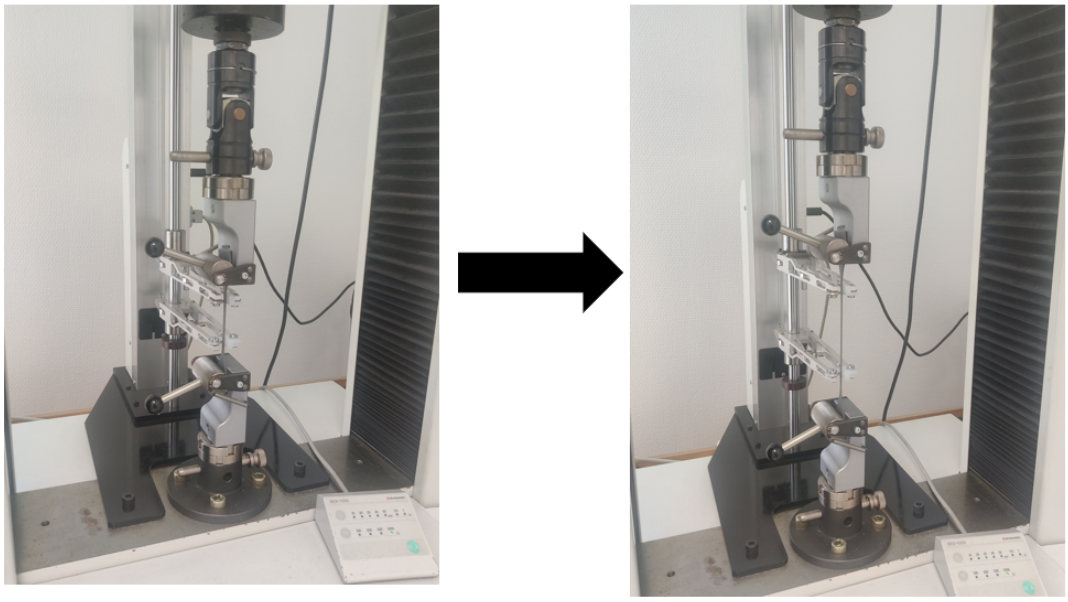

Figure 3.14: overview of testing tensile strength

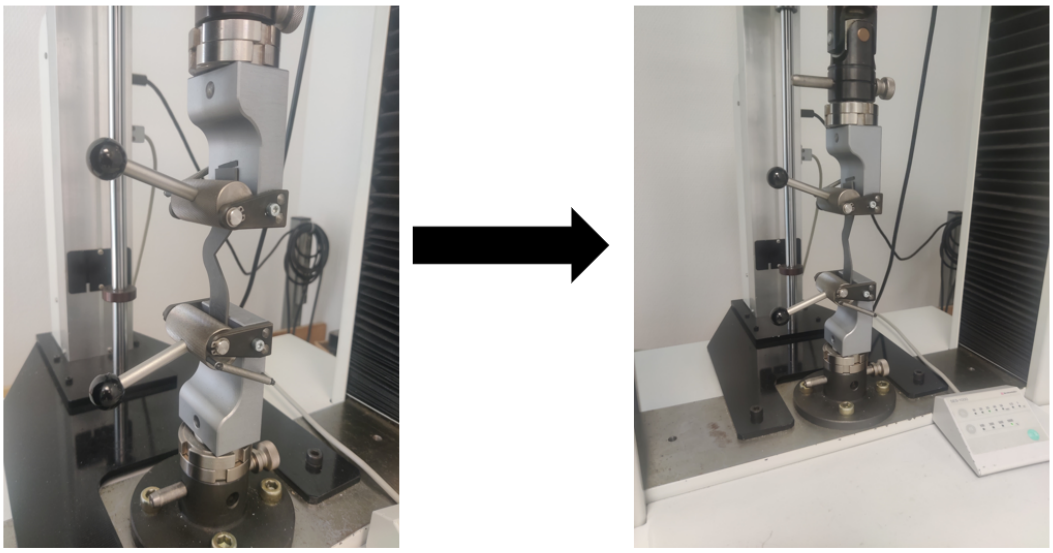

Figure 3.15: overview of testing tear strength

To measure tensile strength, put the cleaned sample between two holders like in Figure 4.14. On the computer, choose the tensile strength test program, specify the folder where data has to be saved and then start the test. The sample will stretch until it breaks, and the program will stop automatically. The test results are saved in a specific folder on the computer. For tear strength, follow the same steps, but use a different program and a differently shaped sample, as shown in Figure 3.15.

4
Results and Discussions

4.1 Electrical properties

4.1.1 DC conductivity (initial screening)

The normalized conductivity of various materials after 1 hour of applying 1 kV at 25°C and 90° are shown in Figures 4.1 and 4.2, respectively. Experimental analysis indicates that it takes about 1 hour for the samples to reach a steady state, so the conductivity is measured at that point. The normalization is done by dividing the conductivity values at each temperature by the reference conductivity at 25°C.

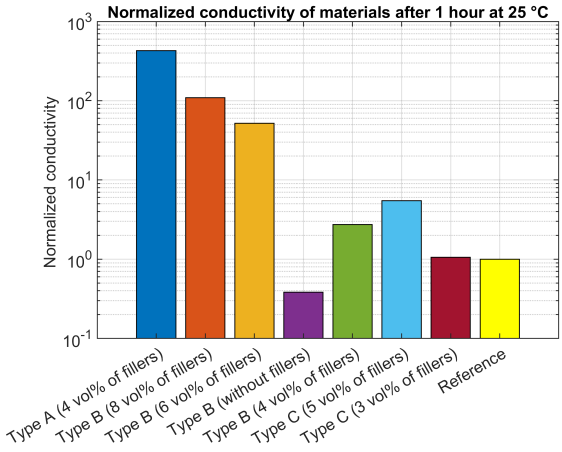

Figure 4.1: Normalized Conductivity of materials after 1 hr at 25°C

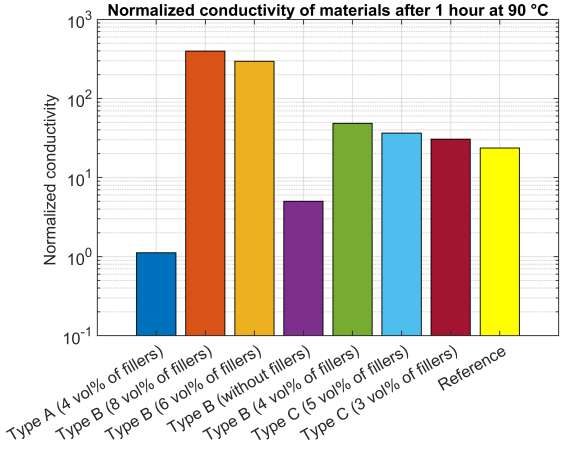

Figure 4.2: Normalized Conductivity of materials after 1 hr at 90°C

From the above figures (figures 4.1 and 4.2) it is clear that the conductivity of most materials at 90°C is higher than at 25°C, except for Type A with 4 vol% of fillers. As the temperature increases, materials gain thermal energy, which excites charge carriers from the valence band to the conduction band, creating more free charge carriers for conduction. However, for Type A with 4 vol% of carbon black fillers, if the polymer matrix (EPDM) and carbon black fillers were expand at different rates when heated. This uneven expansion could potentially disrupts the alignment of conductive fillers, leading to increasing resistance and reducing conductivity. Therefore, Type A with 4 vol% of fillers does not show expected temperature dependency which makes it a not good candidate for field grading material in cable accessories.

The next material, Type B with mica flakes fillers, has irregularly shaped flakes that create more contact points and higher contact resistance. Type B with 8 vol% of fillers has conductivity over two orders of magnitude higher than the reference values. We decided to reduce the filler concentration to 6 vol%, which still shows higher conductivity at both temperatures. However, reducing filler concentration makes the conduction path more roundabout, increasing contact resistance and reducing conductivity.

Next, testing is done with Type B without secondary fillers, but the conductivity was below the reference values. Testing with Type B with 4 vol% of fillers showed slightly higher conductivity than the reference value. According to our selection criteria, we need materials with conductivity within one order of magnitude higher compared to reference value and should be not less than that of reference as well. Therefore, we are selecting Type B with 4 vol% of fillers for detailed screening.

Additionally, Type C- with carbon black fillers (5 vol% and 3vol%) shows good conductivity within our selection criteria, so we are also choosing them for detailed screening.

4.1.2 AC properties

4.1.2.1 Permittivity (initial screening)

The normalized permittivity of materials after by applying 1 kV at 25°C and 90°C depicted in below figures 4.3 and 4.4 respectively. The normalization is done by dividing the permittivity values at each temperature by the reference permittivity at 25°C. The permittivity has to be more than that of the reference value. Higher permittivity can redistributes the electric field more evenly across their volume. This will helps for reducing high field concentrations that can otherwise leads to the dielectric breakdown or insulation failure. From these figures, it is clear that all the materials showing relatively good permittivities.

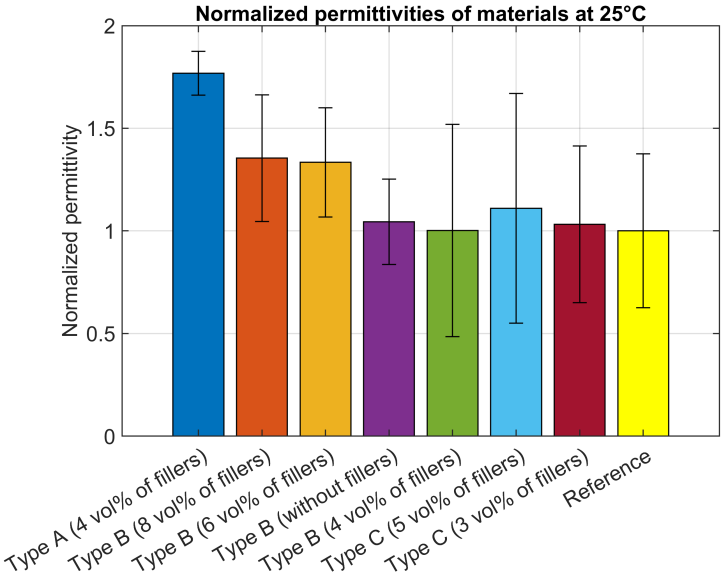

Figure 4.3: Normalized Permittivities of materials at 25°C

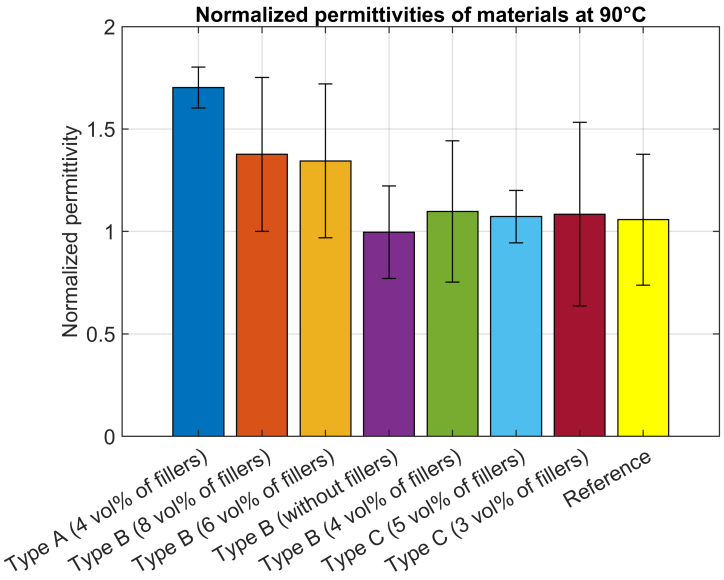

Figure 4.4: Normalized Permittivities of materials at 90°C

4.1.2.2 Dielectric losses (initial screening)

The normalized dielectric losses of materials after applying 1 kV at 25°C and 90°C are shown in Figures 4.5 and 4.6, respectively. The normalization is done by dividing the permittivity values at each temperature by the reference dielectric losses at 25°C. Materials with lower dielectric losses dissipate less heat, so those with dielectric losses equal to or lower than the reference value are considered better. According to the figures, Type B (without fillers), Type C (both 3 vol% and 5 vol% of fillers), and Type B (4 vol% of filler) exhibit lower dielectric losses.

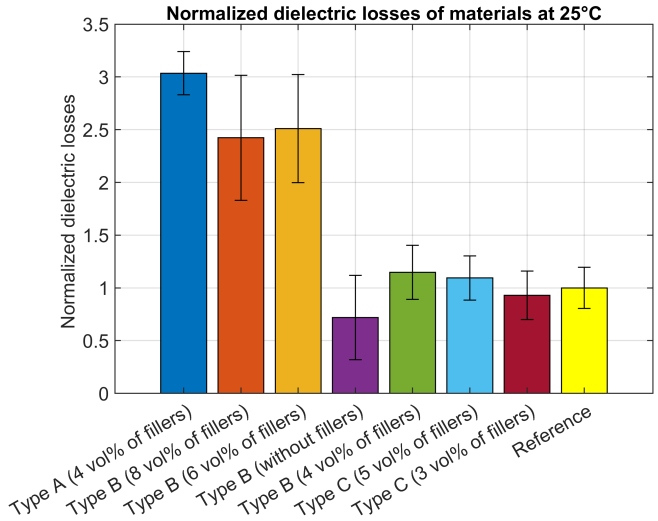

Figure 4.5: Normalized Dielectric losses of materials at 25°C

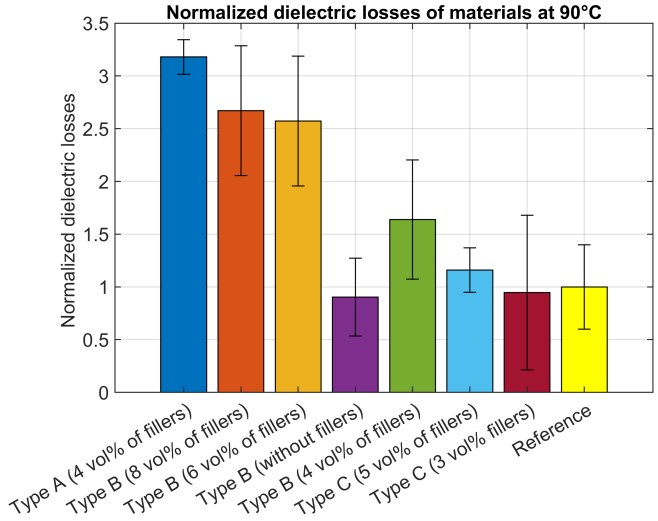

Figure 4.6: Normalized Dielectric losses of materials at 90°C

4.1.2.3 AC breakdown voltage (detailed screening)

Figure 4.7 shows the normalized AC breakdown voltages for materials that performed well in the initial screenings (shows good results by considering candidates selection criteria). The values are normalized by dividing them by the reference AC breakdown voltage.

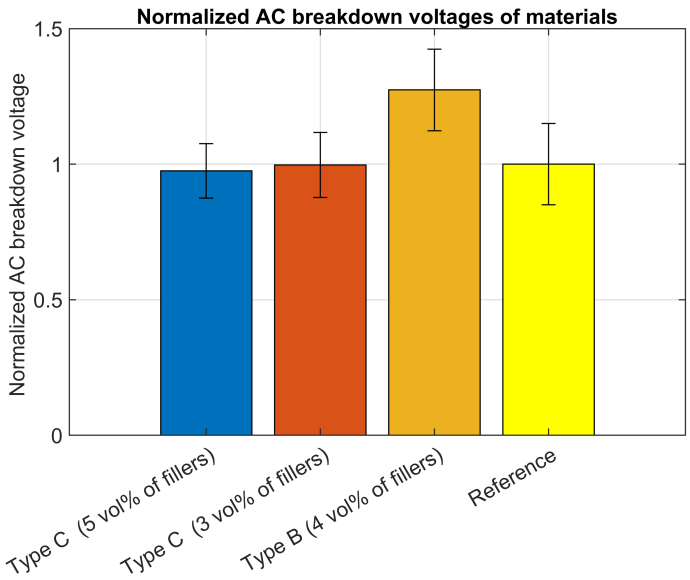

Figure 4.7: Normalized AC breakdown voltages of different materials

Figure 4.7 shows that all three materials have good AC breakdown voltage compared to the reference. However, Type B, which contains 4 vol% of filler, has a slightly higher AC breakdown voltage than the reference. This may because Type B includes mica flakes, and their irregular shape creates more contact points within the material. These extra contact points increase resistance, making it harder for electric charges to move through the material (refer 2.1). As a result, Type B can withstand a stronger electric field before breaking down. On the other hand, materials with carbon black fillers have a more regular shape with fewer contact points, leading to lower resistance and a lower breakdown strength when comparing with material containing 4 vol% of mica flakes.

4.1.3 Nonlinear conductivity measurement (detailed screenig)

The normalized nonlinear conductivity of Type B (4 vol% of fillers) with four different fields is plotted in below figure 4.8. Normalization of conductivities are done by dividing with lowest conductivity of the reference material, and normalization of electric field is done by dividing with the maximum applied field. From the figure, it can be seen that the conductivity of this material at 25°C and 90°C are within 10 times the conductivity of the reference values.

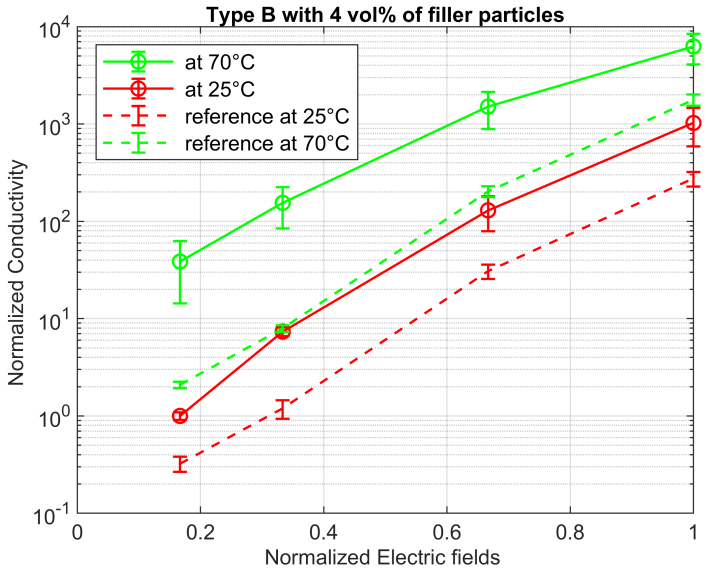

Figure 4.8: Normalized nonlinear Conductivity of Type B (4 vol% of fillers)

Similarly, normalized nonlinear conductivity of Type C (5 vol% of fillers) is plotted in figures 4.9. Normalization is done in the same way as for Type B (4 vol% of fillers). The nonlinear conductivity of Type C with 5 vol% fillers is also within 10 times the reference conductivity values at both temperatures.

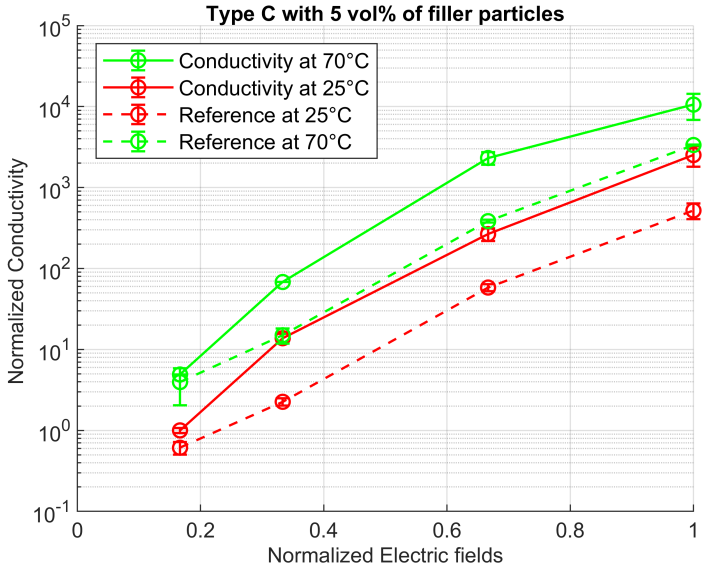

Figure 4.9: Normalized nonlinear Conductivity of Type C (5 vol% of fillers)

Figure 4.10 shows the normalized nonlinear conductivity of Type C with 3 vol% of fillers. Normalization is done by the same way as in the other two candidates. The conductivity of this material is nearly same as the conductivity of the reference material.

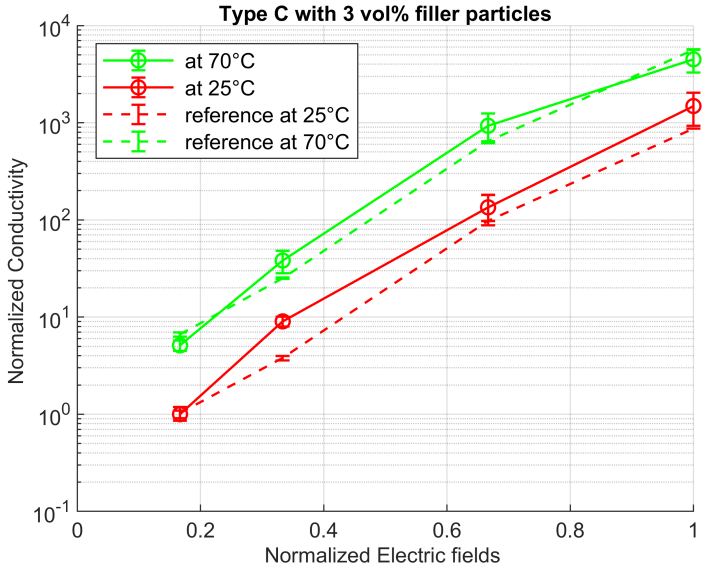

Figure 4.10: Normalized nonlinear Conductivity of Type C (3 vol% of fillers)

The nonlinear conductivity of these materials is used to develop a conductivity model. This model will be applied to investigate the electrothermal simulation of a 525 kV joint under both steady-state and transient conditions.

4.2 Mechanical Properties

The normalized results of the mechanical properties are shown below. All values were normalized by dividing by the corresponding reference values.

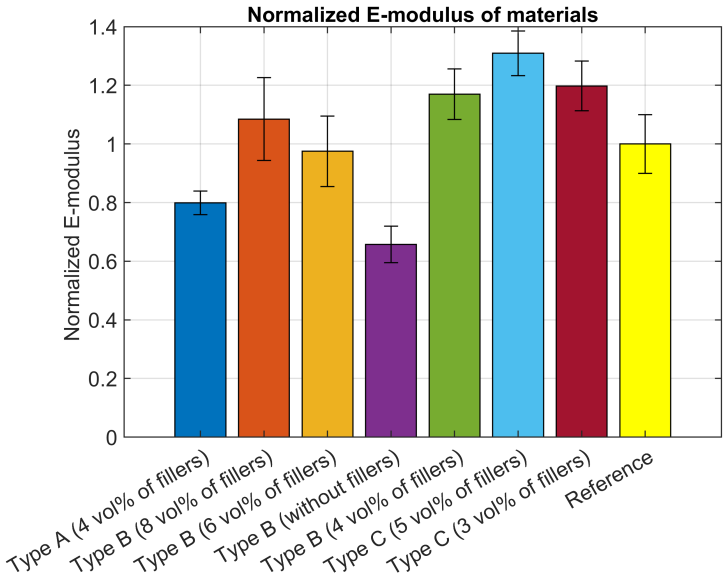

Figure 4.11: Normalized E-modulus of different materials

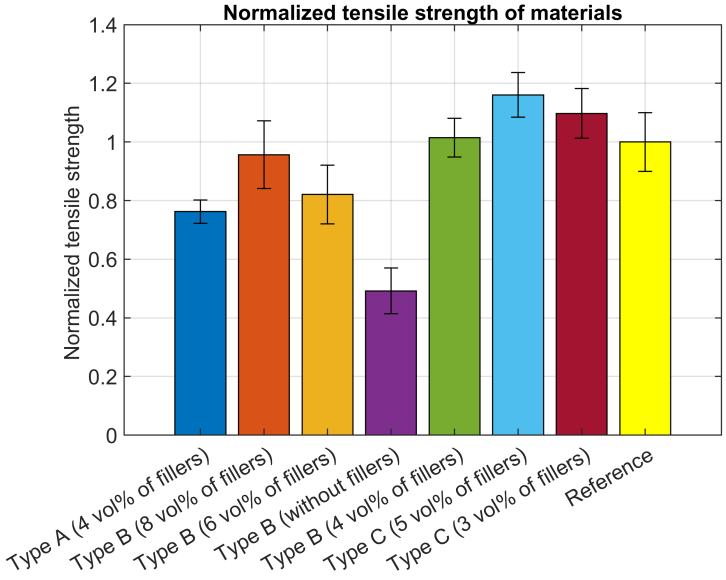

Figure 4.12: Normalized Tensile strength of different materials

Figures 4.11 and 4.12 show bar charts of the normalized E-modulus and tensile strength of various materials, and both charts follow the same trend. Most materials, except Type A (4 vol% of fillers) and Type B (no fillers), have lower E-modulus and tensile strength.For Type B (no fillers), this supports the theory that secondary fillers are needed in FGM to improve mechanical properties. Without these fillers, the mechanical properties are worse. Additionally, Type C (with 5 vol% of fillers), Type C (with 3 vol% of of fillers), and Type B (with 4 vol% of fillers) show relatively good E-modulus and tensile strength compared to the reference material.

If the fillers are does not bond well with the EPDM matrix (weak interfacial bonding), then it cannot reinforce the rubber. This poor bonding leads to the stress transfer between the rubbers and fillers, which reduces the overall stiffness (E-modulas) of the composites.Additionally, the fillers has to be uniformly distributed with the polymer matrix. Poor dispersion can leads to the formation of agglomerates or cluster of the filler particles, which act as stress concentrator. These stress concentrators can initiate the cracks under tensile loading and thereby reducing the tensile strength.

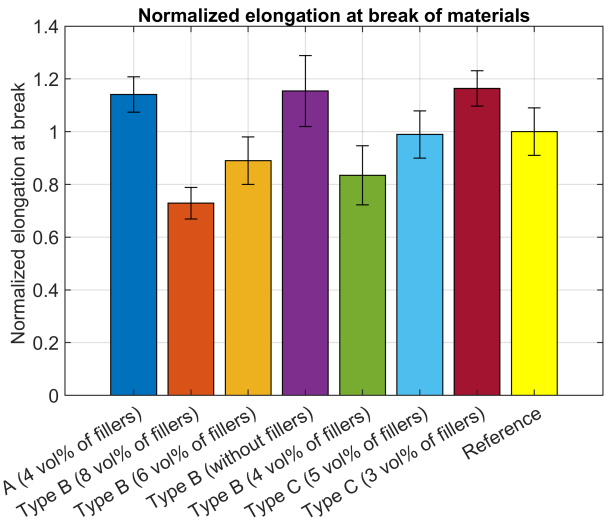

Figure 4.13: Normalized Elongation at break of different materials

Figure 4.13 shows the normalized elongation at break for different materials. Elongation at break increases as filler concentration decreases. Higher filler concentrations make the polymer matrix more rigid and brittle, while reducing filler content maintains the material's natural ductility and flexibility, allowing it to stretch more before breaking. However, Type C with 5% fillers , Type C with 3% fillers , Type A with 4% fillers and Type B without fillers still show relatively good elongation at break compared to the other materials.

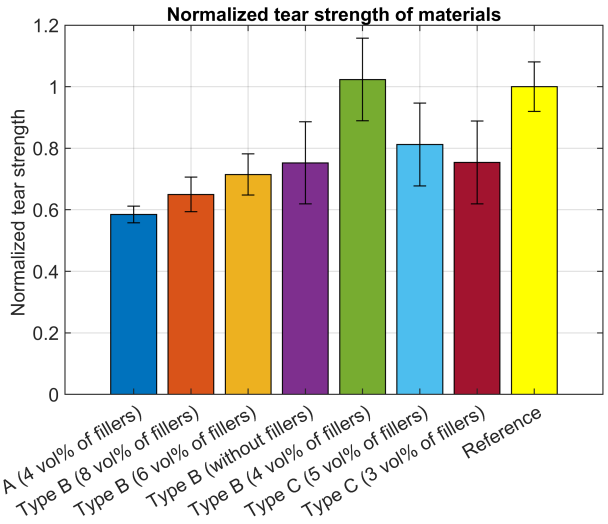

Figure 4.14: Normalized Tear strength of different materials

Normalized tear strength of different materials are plotted in figure 4.14. All the material except Type B (4 vol% of fillers) shows poor tear strength. This is because of fillers can introduce a defect which discontinues the polymer matrix. These can cause the accumulation of stress, makes it easier for initiation of tear .

Overall, all the test has been completed on small scale compounding. the methods used for the mixing and curing can also affect these mechanical properties. That means, inadequate mixing can cause to poor filler dispersion which can adversely impact on the mechanical properties.

5

Simulation

Figure 5.1 illustrates the joint geometry used in the simulation, detailing all the main components. The model includes a cable end with a conductor, cable insulation, and a connector. The insulation is made of cross-linked polyethylene (XLPE). The joint features inner and outer deflectors made of conductive rubber, along with a field grading material (FGM) composed of nonlinear ethylene propylene diene monomer (EPDM). Additionally, EPDM is used as the base polymer for the material in the joint body.

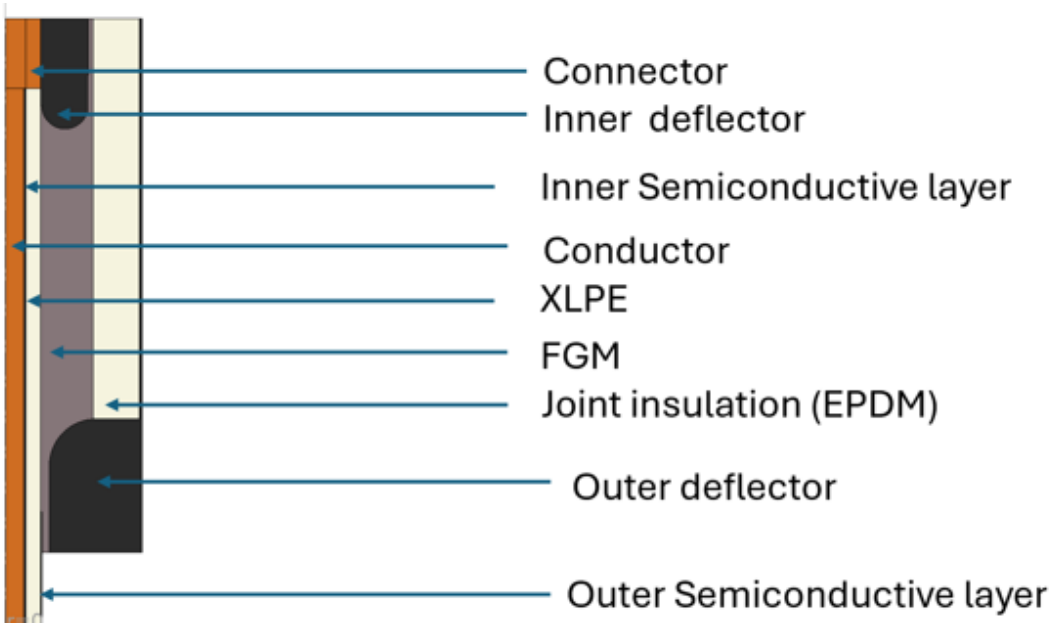

Figure 5.1: 525 kv HVDC cable joint with labelled parts

5.1 simulation cases

The simulation includes both steady state and transient simulations. The steady state simulation includes $U_0 = 525\,\text{kV}$ and a type test voltage of $U_T = 1.85 \times U_0$ [25]. The conductor temperature is set as 70°C.
Additionally, transient simulation of superimposed LIOP (Lightning Impulse Opposite Polarity) were done.The wave shape of superimposed LIOP is given in below figure 5.2 [20] . The maximum voltage of LIOP is $U_{p1} = 2.1 \times U_0 = 1103\,\text{kV}$.

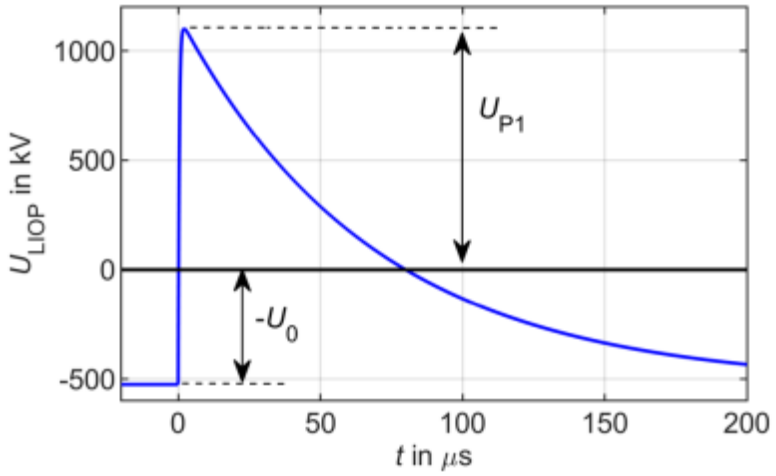

Figure 5.2: Shape of superimposed LIOP [20]

5.2 FGM, XLPE and EPDM properties

In order to add nonlinear electric field dependency of of different field grading materials a mathematical model has to be used. The equation 5.1 [20] below shows the conductivity model representation of FGM .

$$\sigma_{\text{FGM}}(E,T) = \frac{\sigma_{0,\text{FGM}}\left(1+\left(\frac{E}{E_b}\right)^P \exp(\alpha T)\right)}{1+\left(\frac{\sigma_{0,\text{FGM}}}{\sigma_\infty}\right)\left(1+\left(\frac{E}{E_b}\right)^P \exp(\alpha T)\right)} \tag{5.1}$$

where:

$\sigma_{\text{FGM}}(E,T)$ is the Conductivity of FGM dependent on E and T
$\sigma_{0,\text{FGM}}$ is the Base conductivity
E is the Applied electric field
E_b is the Switching field
P is the nonlinearity exponent
α is the temperature coefficient
T is the Temperature
σ_∞ is the Saturation conductivity

The normalized fitting curve for all the materials based on equation 5.1 are plotted in below figure 5.3. The conductivities of different materials are normalized by dividing each material's conductivity value by the corresponding lowest conductivity value at room temperature. Additionally, the electric field is normalized by dividing each field value by the maximum electric field.

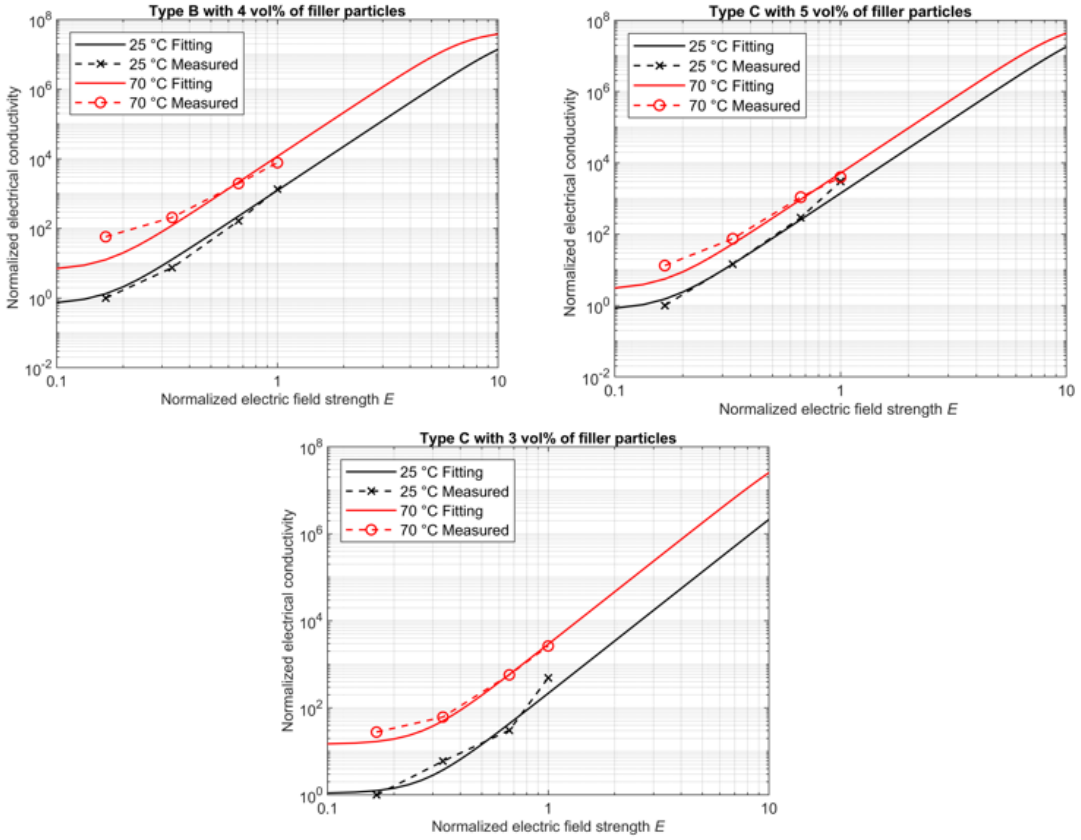

Figure 5.3: Normalised fitting curve for the all the materials

The table below 5.1 the normalized parameters used for the fitting curve modelling. Normalization is done by dividing each parameter by corresponding parameter from the reference values.

Name of material	$\sigma_{0,\mathrm{FGM}}$	σ_∞	$\mathbf{E_b}$	p	α
Type B(4 vol% of fillers)	4	1	1.6	0.76	0.83
Type C(5 vol% of fillers)	5	1	1.6	0.76	0.33
Type C(3 vol% of fillers)	2	1	1	0.72	0.66
Reference material	1	1	1	1	1

Table 5.1: Normalized Conductivity parameter for different materials

.

The normalized conductivities of various materials are plotted in figure 5.4 using equation 5.1 and the parameters from table 5.1. The normalization is done by dividing the conductivity of each material by the conductivity of the reference material at the lowest field. These conductivites are plotted at room temperature.

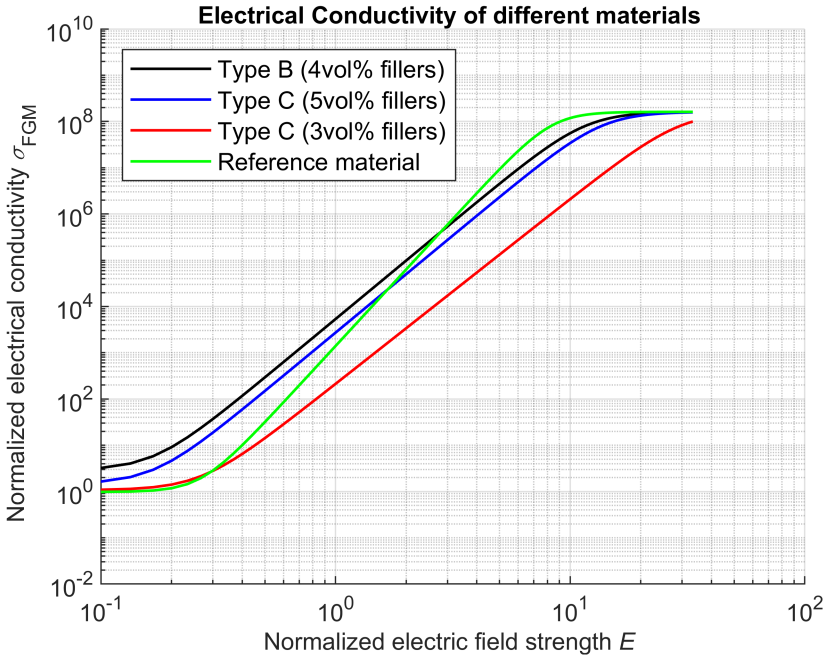

Figure 5.4: Normalised conductivity of materials based on equation 5.1

The normalized electrical conductivity of XLPE and EPDM based on the equation 5.2 and parameters from table 5.2 are plotted in figure 5.5. Normalization of conductivities are done by dividing it with lowest conductivity value, while normalization of electric field is done by dividing with maximum applied field.

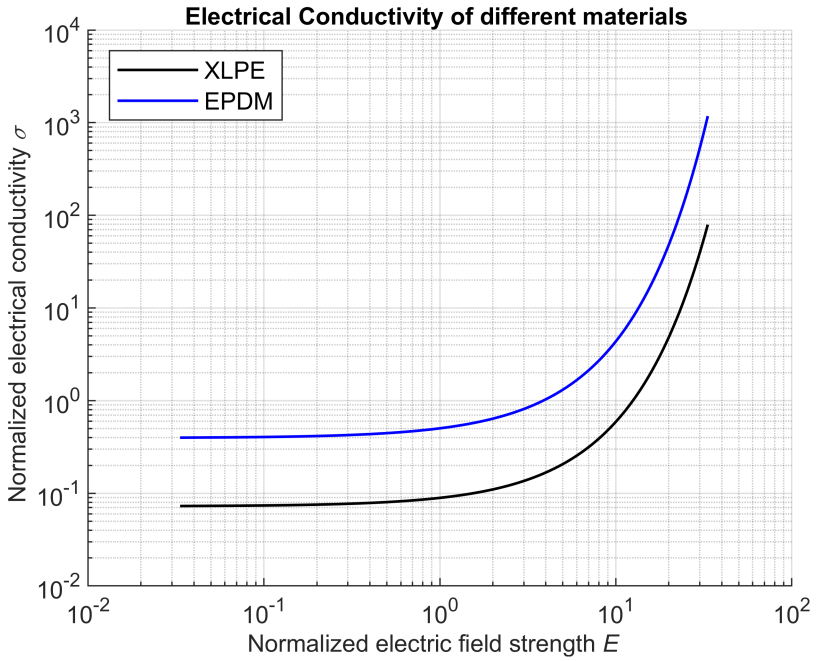

Figure 5.5: Normalized conductivity of materials based on equation 5.2

$$\sigma = \sigma_0 \cdot \exp(\alpha \cdot T + b \cdot E) \tag{5.2}$$

where:

σ_0 is the Base conductivity (S/m)
α is the Temperature coefficient (1/°C)
T is the Temperature (°C)
b is the Electric field coefficient (1/V/m)
E is the Electric field strength (V/m)

Name of material	$\boldsymbol{\sigma_{0,\mathrm{FGM}}}$	$\boldsymbol{\alpha}$	**b**
XLPE	1	1	1
EPDM	3	1.4	1.14

Table 5.2: Normalized Conductivity parameter for different materials

The normalized permittivity of different materials are plotted in table 5.3. the normalisation is done by dividing by the permittivity of reference FGM.

Name of material	**Permittivity**
Type B(4 vol% of fillers)	1.2
Type C(5 vol% of fillers)	1.36
Type C(3 vol% of fillers)	1.18
XLPE	0.41
EPDM	0.49
Reference FGM	1

Table 5.3: Normalized Permittivity of different materials

Figure 5.4 shows that all the materials have a higher base conductivity than XLPE and EPDM (as seen in Figure 5.5), which is crucial for achieving resistive field grading during DC operations. Additionally, the nonlinear increase above the switching field will help to get resistive field grading along with refractive field grading during transient events like lightning and switching impulses. This means that electric stresses are shifted from materials with higher permittivity to those with lower permittivity.

An initial state for temperature and electric field must be defined before applying the transient field. In COMSOL, this approach simplifies the process of defining lightning impulse on top of the DC simulation to get LIOP. It can be done by setting the previously performed DC simulation under $-U_0$ as the initial value of temperature and electric field. The physics used for the simulations are electric currents and heat transfer in solids.

There is no additional losses are considered during simulations. The main purpose of simulation is to understand the performance of material in DC steady sates and transient LIOP operation. The high voltage and ground potential are applied as shown in the figures 5.6 and 5.7 respectively. High voltage is applied across inner deflector and inner semiconductive layer. However ground potential is applied across outer semiconductive layer, outer deflector and external boundary of joint insulation (EPDM).

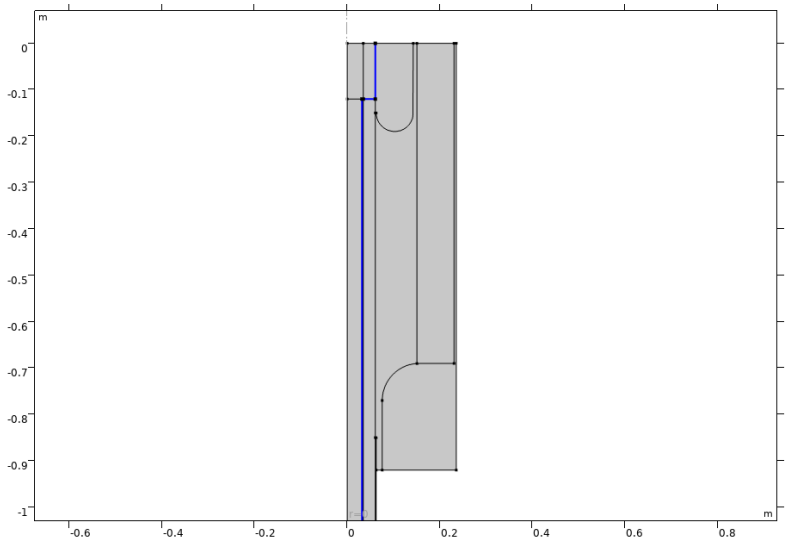

Figure 5.6: high voltage

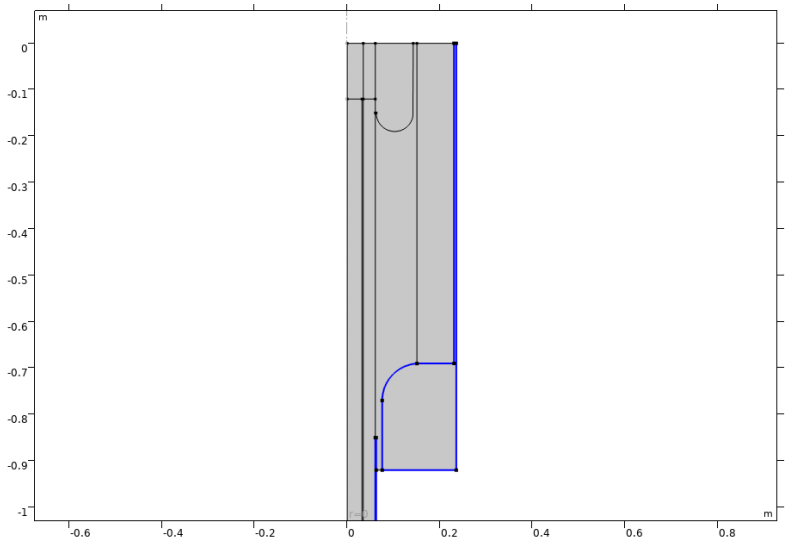

Figure 5.7: ground potential

Figure 5.8 highlights the interfaces for simulations. These simulations primarily examine three key areas: the interface between XLPE and FGM , the interface between FGM and EPDM , and the boundary around the high voltage deflector. These interfaces are crucial because they significantly influence the performance and reliability of the materials under high voltage conditions. Detailed results and analyses of these simulations will be provided in the next chapter, where the impact of these interfaces on electric field distribution and material behavior under various operating conditions will be thoroughly discussed.

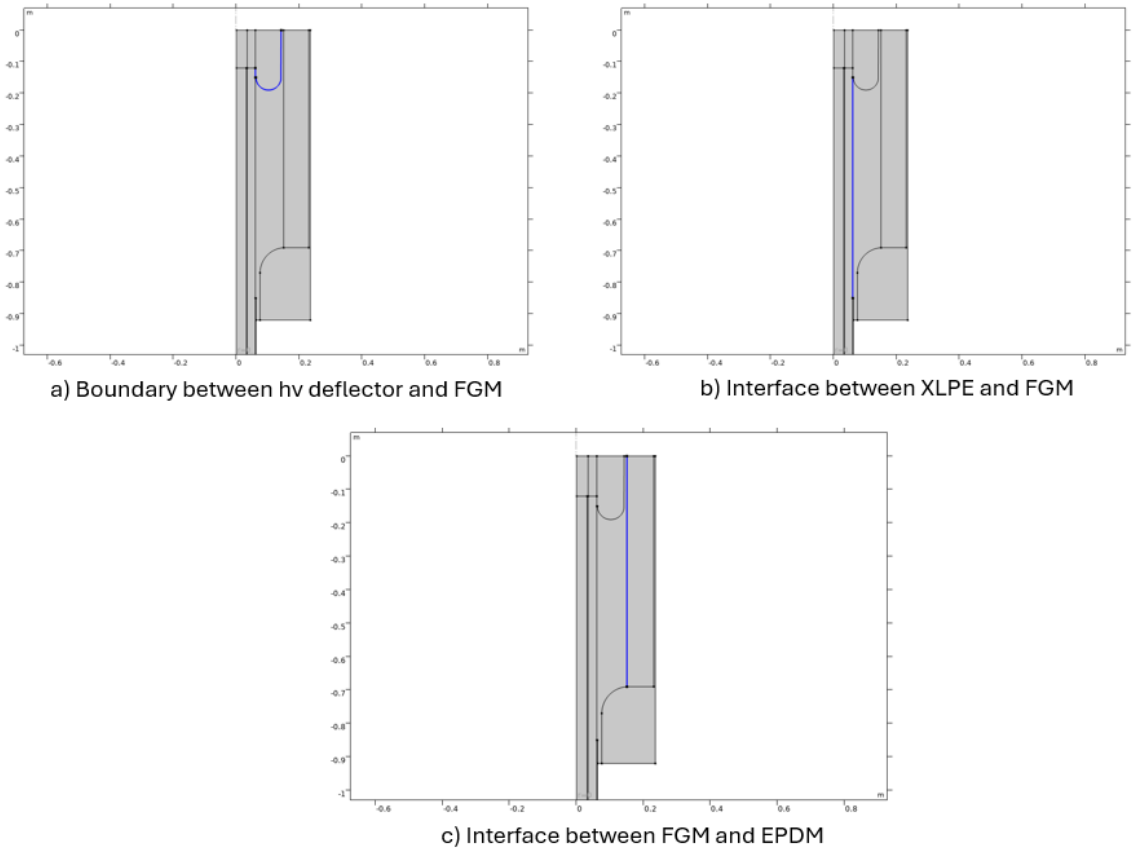

Figure 5.8: illustration of interfaces used for evaluation of simulation

5.3 Simulation result and discussions

The normalized electric field distribution for Type C (with 3 vol% of fillers) at different voltages is described below. Normalization is done by dividing by the maximum electric field strength within the FGM. This simulation focuses on the electric stress in the FGM, EPDM, and deflectors, so all other domains are not selected.

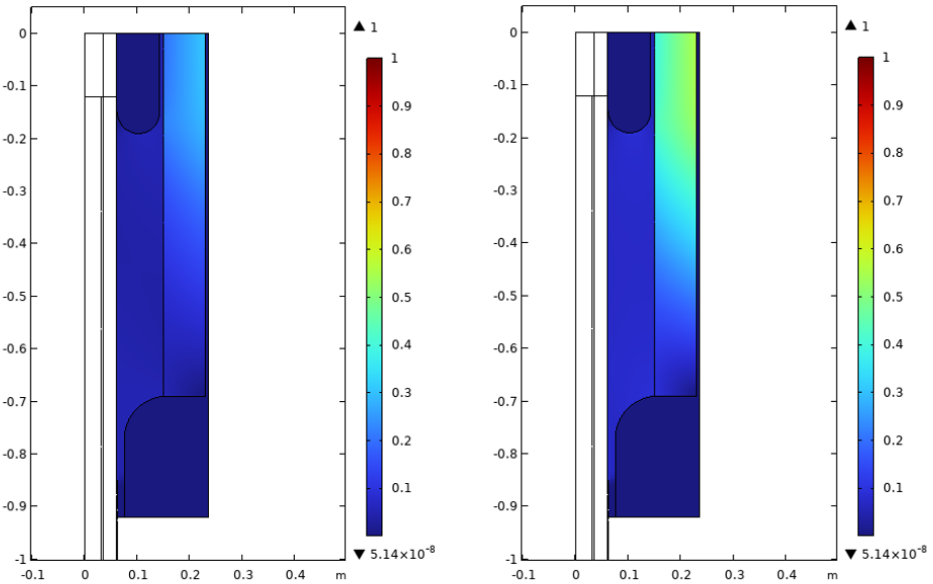

Figure 5.9: Normalised electric field distribution under DC for Type C(3vol% of fillers)

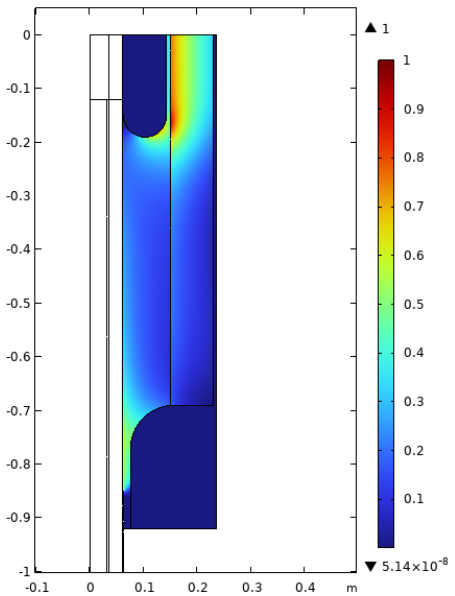

Figure 5.10: Normalized electric field distribution at peak voltage of LIOP for Type C(3vol% of fillers)

Figure 5.9 shows that the electric stress within the FGM is evenly distributed, which is crucial for regions like the cable-joint and XLPE-EPDM interfaces. Figures 5.4 and 5.5 reveal that Type C (with 3 vol% of fillers) has slightly higher conductivity than EPDM, causing the electric stress to move from the FGM to the EPDM, resulting in a more uniform stress distribution in the FGM.

Figure 5.10 displays the electric stress distribution at the peak voltage of LIOP (at t=2 µs). Since LIOP is a superimposed voltage (as shown in Figure 5.2), the initial solution at 0 seconds for LIOP matches that of Figure 5.9(a). This leads to a combination of resistive and refractive field grading, concentrating more stress in the EPDM part. This shift occurs because the permittivity of FGM (Type C with 3 vol% of fillers) is higher than that of EPDM, as indicated in table 5.3. Therefore, during this transient case, stress shifts from FGM to EPDM.

Additionally, Figure 5.9 shows field inversion can be seen in EPDM for both U_0 and U_T cases, means that the electric stress near the high voltage deflector is lower compared to EPDM. This occurs because temperature-dependent conductivity causes electric stress to move from higher to lower conductivity (in EPDM) whenever there is a temperature drop between the high voltage deflector and ground potential. However, this is not observed in LIOP (figure 5.10) due to the capacitive field, which is independent of temperature-dependent electric conductivity.

Figure 5.11 shows the normalized electric stress distribution at the peak voltage of LIOP at the boundary between the high voltage deflector and FGM for all materials. Normalization is done by dividing by the highest electric stress of the reference material.

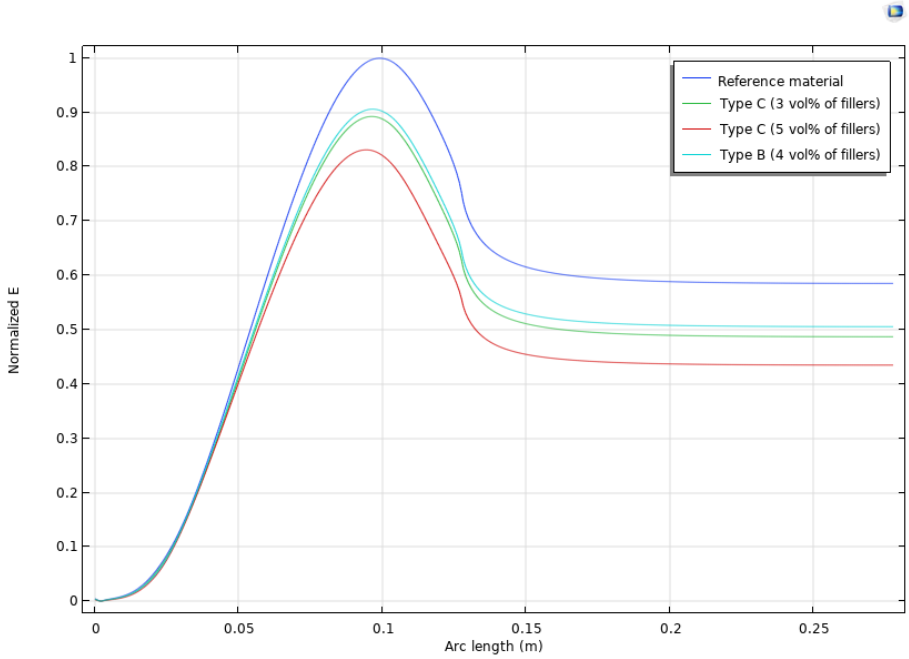

Figure 5.11: Normalized electric stress distribution at the peak voltage of LIOP at the boundary between the high voltage deflector and FGM

Figure 5.11 shows that Type C (with 5 vol% of fillers) has 20% lower peak electric stress, while Type B (with 4 vol% of fillers) and Type C (with 3 vol% of fillers) have a 10% lower peak electric stress at the boundary between the high voltage deflector and FGM when compared to the reference material. It is because of Type C (with 5 vol% of fillers) has higher permittivty when compare with Type C (with 3 vol% of fillers) and Type B (with 4 vol% of fillers) (refer table 5.3).

Figure 5.12 shows the normalized tangential electric field stress for U_0 at the FGM-XLPE interface. The normalization is done by dividing by the maximum field strength of the reference material.

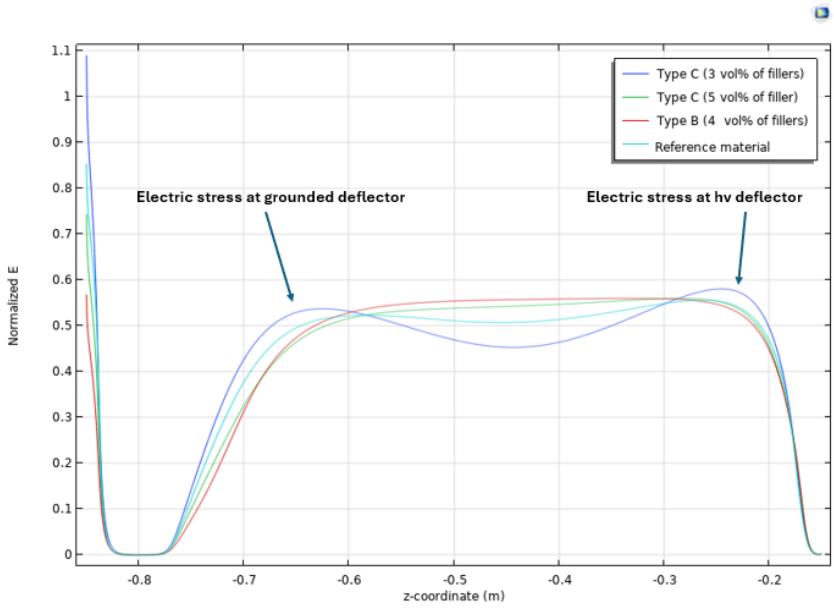

Figure 5.12: Normalized tangential electric stress for U_0 at FGM-XLPE interface

In the left part of Figure 5.12, there is a sudden increase in the electric stress, which is caused by meshing issues (mesh singularity). Type C (with 3 vol% of fillers) shows more uneven field distributions when compare with other materials. The left side peak of Type C (with 3 vol% of fillers) indicates the stress at the grounded deflector, and on the right side peak denotes the stress at the high voltage deflector. These peaks cannot be seen in other materials. It is because of capacitive field distribution is more dominating over resistive field distribution in this Type C (with 3 vol% of fillers). However, Type C (with 5 vol% fillers) ,Type B (with 4 vol% fillers) and reference materials shows more even field distribution at FGM-XLPE interface under U_0.

Figure 5.13 shows the normalized electric stress for U0 at the FGM-EPDM interface (inside the FGM). The normalization is done by dividing by the maximum field strength of reference material. The left side peak of the graphs indicates the highest electric stress at the grounded deflector, while the right side peak shows the highest stress at the high voltage deflector. Type C (3 vol% of fillers) has highest electric stress at both deflectors, while Type B (4 vol% of fillers) and Type C (5 vol% of fillers) have lower stresses at deflectors and shows more even stress distribution. This is because Type C (3 vol% of fillers) has lower conductivity which leads to higher electric field strength (refer figure 5.4).

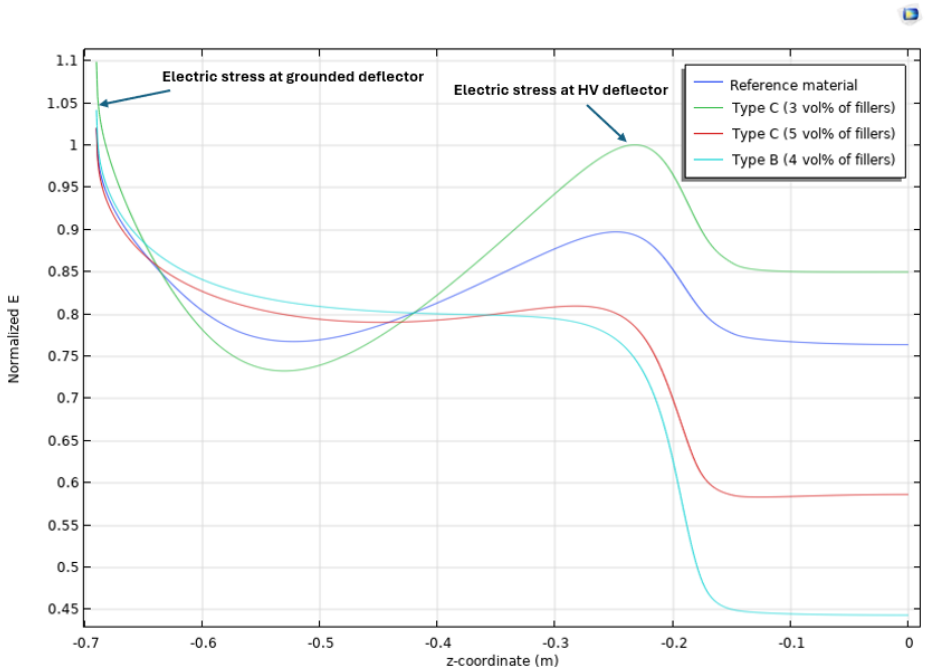

Figure 5.13: Normalised electric stress for U_0 at FGM-EPDM interface (inside FGM)

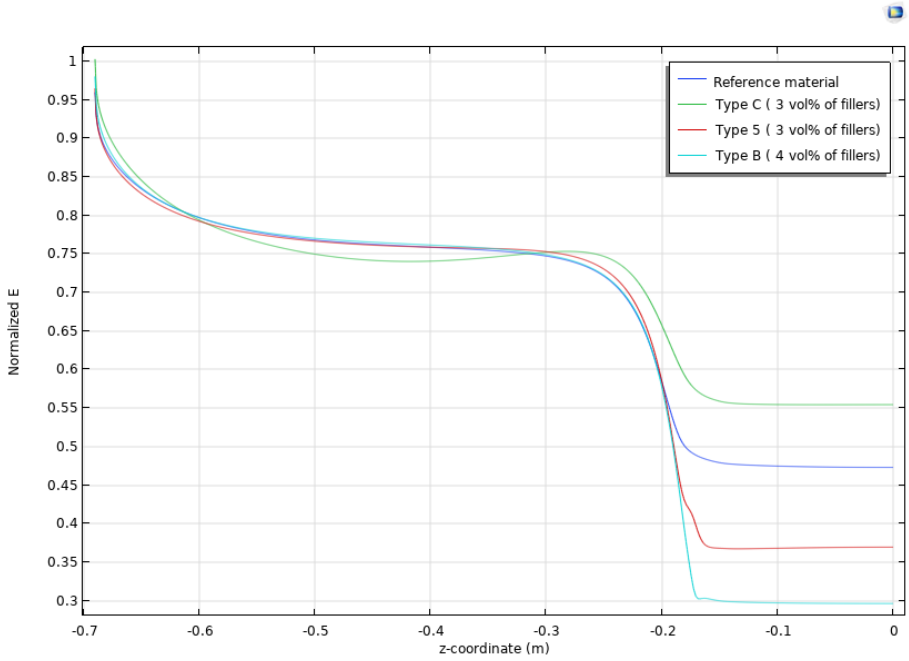

Figure 5.14: Normalized electric stress for U_T at FGM-EPDM interface (inside FGM)

Figure 5.14 shows the normalized electric stress for U_T at the FGM-EPDM interface (inside the FGM). The normalization is done by dividing by the maximum field strength of reference material. The field distribution from the ground deflector to high voltage deflector is similar for all FGMs compared to the reference. However, there is a difference in the stress distribution above the high voltage deflector. Materials with higher conductivity have lower electric fields refer figure 5.4. Therefore, Type B (4 vol% of fillers) and Type C (5 vol% of fillers) shows lower stress compare to Type C (3 vol% of fillers).

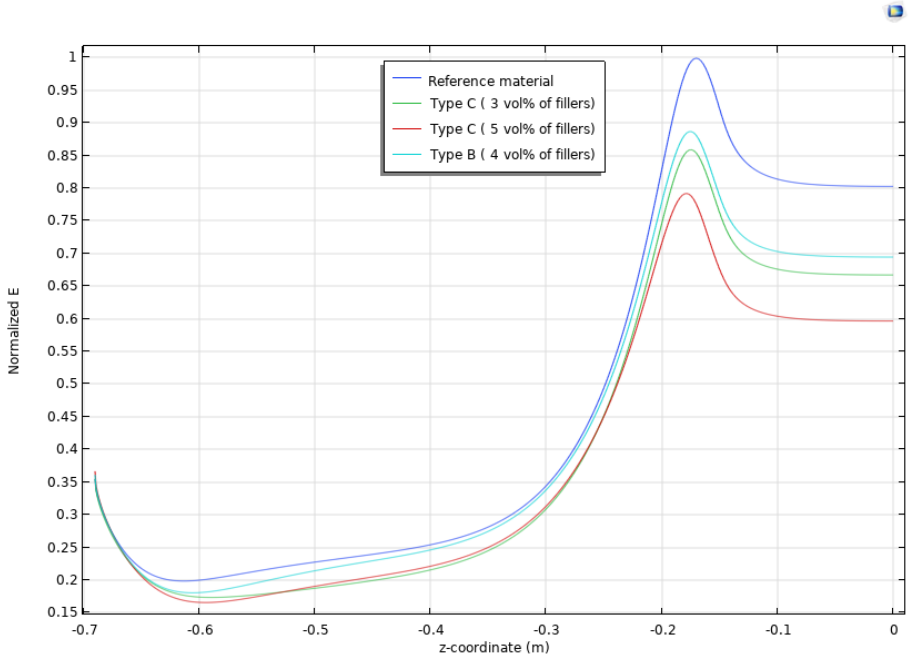

Figure 5.15: Normalized electric stress for LIOP at FGM-EPDM interface (inside FGM)

Figure 5.15 shows the normalized electric stress for peak voltage of LIOP at the FGM-EPDM interface (inside the FGM). The normalization is done by dividing by the maximum field strength of reference material. The reference material has the highest electric stress at the high voltage deflector. However, Type C (5 vol% of fillers) has lower electric stress compared to the other materials. It is because of higher permittivity of Type C (5 vol% of fillers) when compared to other materials (refer table 5.3).

Figure 5.16 shows how the electric stress is distributed at the FGM-EPDM inside EPDM interface inside EPDM when U_0 is applied. The normalization is done by dividing by the maximum field strength of Type C (3 vol% of fillers). Since FGMs have higher conductivity than EPDM (as shown in Figures 5.4 and 5.5), the electric stress moves from the FGM to the EPDM. This results in higher stress in the EPDM, but it doesn't cause the EPDM to break down. This means EPDM has a much higher breakdown strength compared to FGM. The lower stress is present in Type C (3 vol% of fillers) (refer figure 5.13). In general, if there's less stress in the FGM, more stress shifts to the EPDM, and the EPDM can handle it.

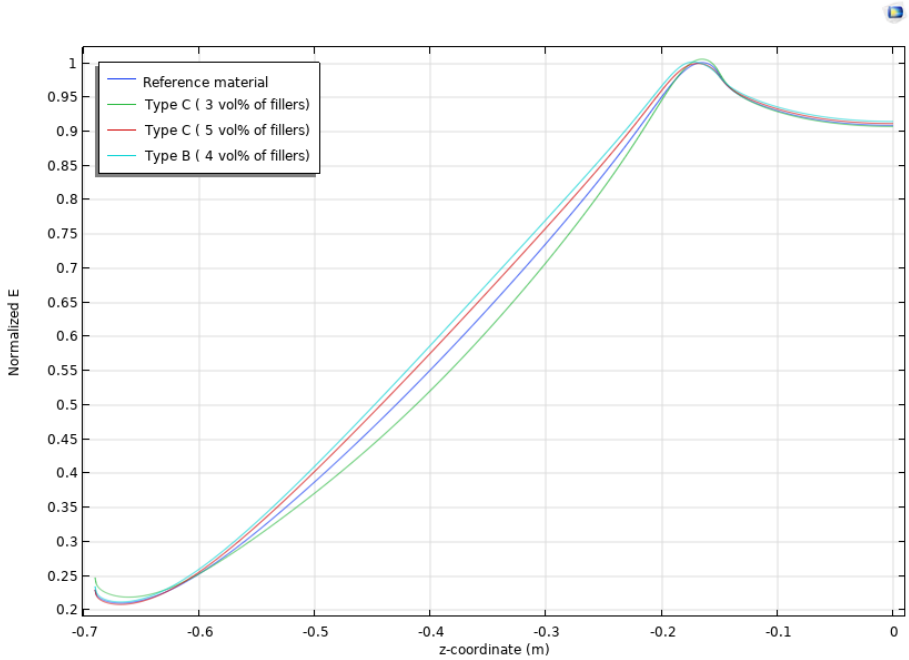

Figure 5.16: Normalized electric stress for U_0 at FGM-EPDM interface (inside EPDM)

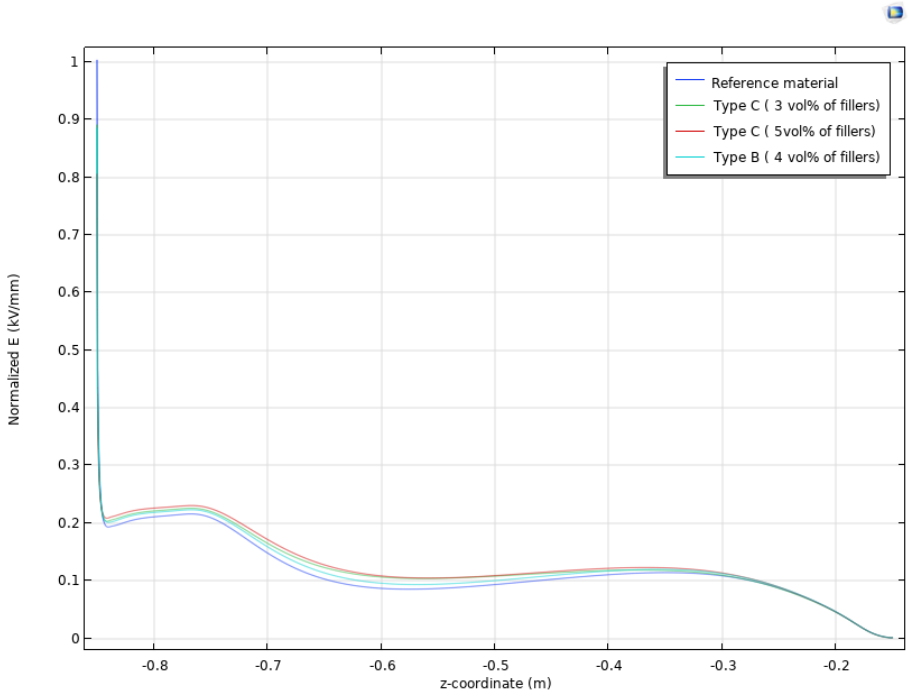

Figure 5.17: Normalized electric stress for LIOP at XLPE-FGM interface (inside XLPE)

Figure 5.17 shows the normalized electric stress for the maximum voltage of LIOP at the XLPE-FGM interface (inside the XLPE). The stress is normalized by dividing by the maximum field strength of the reference material. Since FGM has higher conductivity than XLPE, the electric stress shifts from the FGM to the XLPE. Like EPDM, XLPE has much higher breakdown strength. In this figure, Type C (5 vol% of fillers) has higher electric stress than the other materials, which means it experiences less stress in the FGM at the same interface for LIOP.

6

Conclusion

Aim of thesis work was to investigate impact of secondary fillers on electrical and mechanical properties in FGM. Finally, electrothermal simulations were performed on a 525 kV cable joint. The measured nonlinear conductivity was fitted to a mathematical model and assigned to the field grading material (FGM) in the cable joint model used in COMSOL Multiphysics..

The testing process is divided into two stages: initial screening and detailed screening. During the initial screening, tests are conducted to measure conductivity, permittivity, dielectric loss, and mechanical properties such as elastic modulus, tensile strength, elongation at break and tear strength. Detailed screening is only carried out if the conductivity measurements from the initial screening are within one order of magnitude of the conductivity from the reference material (refer 2.20). The detailed screening involves measuring the AC breakdown strength and the nonlinear conductivity of the selected materials. The initial electrical screening shows that Type B with 4 vol% of mica flake fillers, Type C with 5 vol% and 3 vol% of carbon black fillers have good electrical conductivities and AC properties which strictly follows the material selection criteria (refer table 2.3). However, other materials like Type A with 4 vol% of fillers, Type B with 8 vol% and 6 vol% of fillers showing good permittivities (refer 4.3 and 4.4), but poor dielectric losses (refer 4.5 and 4.6) and DC conductivities (refer 4.1) and (refer 4.2). The mechanical results shows that Type B with 4 vol% of mica flakes fillers, Type C with 5 vol% and 3 vol% of carbon black fillers follow candidates selection criteria and showing good results at E-modulus (refer 4.11)and tensile strength (refer 4.12). However, elongation at break of Type B with 4 vol% of mica flakes fillers are low when compared with Type C with 5 vol% and 3 vol% of carbon black fillers. Additionally, non of the materials except Type B with 4 vol% of mica flakes fillers shows good tear strength. Additionally, the tests were done on materials made from small-scale compounding which can lead to uneven filler distribution. This uneven filler distribution could result in bigger batch to batch variation for electrical and mechanical properties.

The detailed screening revels that, AC breakdown voltage of Type B with 4 vol% of mica flake fillers, shows good results when compared with Type C with 5 vol% and 3 vol% of carbon black fillers, based on selection criteria (refer 4.7). This is because Type B contains mica flakes fillers, which create more contact points between the fillers. This makes it harder for electric charges to pass through the material, leading to a higher breakdown voltage. Additionally, the nonlinear conductivity of these materials is also within one order of magnitude of the reference value (refer 4.8, 4.9 and 4.10).

Simulations were performed for both normal DC voltages and transient voltages at different interfaces (refer 5.8). The simulation results shows that Type C with 5 vol% of carbon black fillers experiences lower electrical stress at boundary between the HV deflector and FGM under LIOP voltage (refer 5.11). Additionally, the electric fields are more evenly distributed in Type C with 5 vol % of fillers and Type B with 4 vol% of mica flake fillers at various locations and voltages compared to the other two materials (refer 5.12, 5.13, 5.14 and 5.15). Additionally, the current simulations did not account for losses, so future simulations should include both polarization and conduction losses.
Overall, electrical and mechanical tests were conducted on 1mm and 2mm samples, respectively. Therefore, testing high voltage cable joints with bulk quantities of these materials is needed and can be considered for future work.

This thesis work shows that from small scale compounding, Type B with 4 vol% of mica flake fillers and Type C with 5 vol% and 3 vol% of carbon black fillers shows a good balance between mechanical and electrical properties. As compounding technique impact both electrical and mechanical properties significantly, compounding on a larger scale is required to further evaluate stability of properties with specific filler concentration.

Bibliography

[1] G. Lagrotteria, D. Pietribiasi and M. Marelli, "HVDC Cables - The technology boost," 2019 AEIT HVDC International Conference (AEIT HVDC), Florence, Italy, 2019, pp. 1-5, doi: 10.1109/AEIT-HVDC.2019.8740645. keywords: Cable insulation;Space charge;HVDC transmission;Conductivity;Soil;Land surface temperature;HVDC Cables;XLPE;HPTE.

[2] A. Küchler, 2018, High Voltage Engineering: Fundamentals – Technology – Applications, Springer Verlag, Schweinfurt, Germany.

[3] E. Kuffel, W.S. Zaengl, J. Kuffel, Chapter 4 - Electrostatic fields and field stress control, Editor(s): E. Kuffel, W.S. Zaengl, J. Kuffel, High Voltage Engineering Fundamentals (Second Edition), Newnes, 2000, Pages 201-280, ISBN 9780750636346, https://doi.org/10.1016/B978-075063634-6/50005-8. (https://www.sciencedirect.com/science/article/pii/B9780750636346500058)

[4] T. Christen, L. Donzel and F. Greuter, "Nonlinear resistive electric field grading part 1: Theory and simulation," in IEEE Electrical Insulation Magazine, vol. 26, no. 6, pp. 47-59, November-December 2010, doi: 10.1109/MEI.2010.5599979. keywords: Finite element methods;Conductivity;Electric fields;Voltage control;Stress;Electrodes;Switches;electric stress control, nonlinear field grading material, finite element simulation;high voltage cable accessory,

[5] Cigré Working Group D1.56, 2020, Field grading in electrical insulation systems, Technical Brochure 794.

[6] Grading electric field in high voltage insulation using composite materialshttps://www.researchgate.net/publication/322260967

[7] M. Secklehner, R. Hussain and V. Hinrichsen, "Tailoring of new field grading materials for HVDC systems," 2017 INSUCON - 13th International Electrical Insulation Conference (INSUCON), Birmingham, UK, 2017, pp. 1-6, doi: 10.23919/INSUCON.2017.8097174. keywords: Conductivity;Cable insulation;Mathematical model;Power cables;Stress;Cable shielding,

[8] Electromagnetic mixing formulas and applications / Ari Sihvola

[9] T. Christen, L. Donzel and F. Greuter, "Nonlinear resistive electric field grading part 1: Theory and simulation," in IEEE Electrical Insulation Magazine, vol. 26, no. 6, pp. 47-59, November-December 2010, doi: 10.1109/MEI.2010.5599979. keywords: Finite element methods;Conductivity;Electric fields;Voltage control;Stress;Electrodes;Switches;electric stress control, nonlinear field grading material, finite element simulation;high voltage cable accessory,

[10] L. Donzel, F. Greuter and T. Christen, "Nonlinear resistive electric field grading Part 2: Materials and applications," in IEEE Electrical Insulation Magazine, vol. 27, no. 2, pp. 18-29, March-April 2011, doi: 10.1109/MEI.2011.5739419.

keywords: Nonlinear systems;Electric fields;Conductivity;electric stress control;nonlinear field grading material;microvaristor,

[11] M. A. Baferani, C. Li, T. Shahsavarian, I. Jovanovic and Y. Cao, "Development of Nonlinear Field Grading Material for Controlling Electric Field in DC Connectors," 2020 IEEE Conference on Electrical Insulation and Dielectric Phenomena (CEIDP), East Rutherford, NJ, USA, 2020, pp. 330-333, doi: 10.1109/CEIDP49254.2020.9437506. keywords: Connectors;Power cables;Silicon carbide;HVDC transmission;Simulation;Power cable insulation;Reliability engineering,

[12] C. Han, B. Du, Z. Li and Z. Yang, "Effect of Mechanical Tensile on Nonlinear Conductivity of Silicon Carbide/Silicone Rubber Composites for Prefabricated Joint of HVDC Cable," 2020 International Symposium on Electrical Insulating Materials (ISEIM), Tokyo, Japan, 2020, pp. 281-284. keywords: Conductivity;Silicon carbide;Electric fields;Cable insulation;Couplings;HVDC transmission;Doping;nonlinear conductivity;prefabricated cable joint;mechanical tensile;SiR;conducting routes,

[13] M. A. Baferani, T. Shahsavarian, C. Li, M. Tefferi, I. Jovanovic and Y. Cao, "Electric field tailoring in HVDC cable joints utilizing electrothermal simulation: effect of field grading materials," 2020 IEEE Electrical Insulation Conference (EIC), Knoxville, TN, USA, 2020, pp. 400-404, doi: 10.1109/EIC47619.2020.9158756. keywords: Electric fields;Power cables;Power cable insulation;Steady-state;Lightning;HVDC cable joint;electrothermal model;field grading material,

[14] Y. Zhang et al., "Optimal Design of Functionally Graded Power Cable Joint Utilizing Silicone Rubber/Carbon Nanotube Composites," in IEEE Access, vol. 9, pp. 123689-123703, 2021, doi: 10.1109/ACCESS.2021.3109487. keywords: Insulation;Power cables;Dielectrics;Conductivity;Power cable insulation;Permittivity;Electric breakdown;Dielectric properties;electric field optimization functionally graded material;polymeric nanocomposites power cable insulation,

[15] B. X. Du, Z. R. Yang, Z. L. Li and J. Li, "Temperature-dependent nonlinear conductivity and carrier mobility of silicone rubber/SiC composites," in IEEE Transactions on Dielectrics and Electrical Insulation, vol. 25, no. 3, pp. 1080-1087, June 2018, doi: 10.1109/TDEI.2018.006942. keywords: Conductivity;Temperature measurement;Silicon carbide;Power cables;Temperature;HVDC transmission;Conductivity measurement;HVDC cables;cable termination;field grading material;nonlinear conductivity;carrier mobility;high-temperature,

[16] D. Seleznev, A. Egupov, G. Greshnyakov and S. Dubitsky, "Combining Resistive and Capacitive Stress Grading in High Voltage Cable Joints," 2021 IEEE Conference of Russian Young Researchers in Electrical and Electronic Engineering (ElConRus), St. Petersburg, Moscow, Russia, 2021, pp. 1539-1543, doi: 10.1109/ElConRus51938.2021.9396152. keywords: Heating systems;Electron tubes;Numerical models;Electric fields;Stress;Testing;Material properties;composite regulatory tube;cable accessories;resistive field grading;capacitive field grading;FEA simulation,

[17] S. Nikolajevic, M. Djurovic, R. Dimitrijevic, N. Kartalovic, D. Rakovic and P. Osmrokovic, "Development of high dielectric constant materials for cable accessories and design of XLPE MV cable terminations," Proceedings of 1994 IEEE International Symposium on Electrical Insulation, Pittsburgh, PA, USA, 1994, pp. 570-573, doi: 10.1109/ELINSL.1994.401391. keywords: High-K gate dielectrics;Dielectric materials;Power cables;Coatings;Stress control;Polyethylene;Power system control;Power systems;Distributed computing;Finite element methods,

[18] T. T. N. Vu, S. L. Roy and G. Teyssedre, "Targeted Thermal and Electrical Properties of Rubber Materials for HVDC Cable Accessories," 2022 IEEE 4th International Conference on Dielectrics (ICD), Palermo, Italy, 2022, pp. 53-56, doi: 10.1109/ICD53806.2022.9863471. keywords: Temperature dependence;Adaptation models;Power cables;HVDC transmission;Power cable insulation;Conductivity;Thermal conductivity,

[19] Wenmin Guo, Rong Zhang, Xiang Lu and Zhonghua Li, "Simulation of transient response characteristics in coaxial electrodes with nonlinear insulating dielectrics," 2009 IEEE 9th International Conference on the Properties and Applications of Dielectric Materials, Harbin, 2009, pp. 1145-1149, doi: 10.1109/ICPADM.2009.5252316. keywords: Transient response;Coaxial components;Electrodes;Dielectrics and electrical insulation;Conductivity;Electric fields;Voltage;Conducting materials;Dielectric materials;Application software;non-linear;transient response;simulation;ElecNet,

[20] Hussain, Rashid. (2023). Electrothermal FEM simulation of relevant test conditions of a 525 kV HVDC cable joint including nonlinear field grading material.

[21] B. X. Du, C. Han and Z. L. Li, "Effect of Mechanical Stretching on Nonlinear Conductivity and Dielectrics Breakdown Strength of SiR/SiC Composites," in IEEE Transactions on Dielectrics and Electrical Insulation, vol. 28, no. 3, pp. 996-1004, June 2021, doi: 10.1109/TDEI.2021.009434. keywords: Electric potential;Silicon carbide;Power cables;Power cable insulation;Mechanical cables;Conductivity;Mechanical factors;mechanical stretching;cable accessories;silicone rubber;SiC;nonlinear conductivity;breakdown strength;trap density,

[22] Sheikh, Md. Rana. (2023). MECHANICAL PROPERTIES OF POLYMERS.

[23] C. Han, B. Du, Z. Li and Z. Yang, "Effect of Mechanical Tensile on Nonlinear Conductivity of Silicon Carbide/Silicone Rubber Composites for Prefabricated Joint of HVDC Cable," 2020 International Symposium on Electrical Insulating Materials (ISEIM), Tokyo, Japan, 2020, pp. 281-284. keywords: Conductivity;Silicon carbide;Electric fields;Cable insulation;Couplings;HVDC transmission;Doping;nonlinear conductivity;prefabricated cable joint;mechanical tensile;SiR;conducting routes,

[24] W. S. Zaengl, "Dielectric spectroscopy in time and frequency domain for HV power equipment. I. Theoretical considerations," in IEEE Electrical Insulation Magazine, vol. 19, no. 5, pp. 5-19, Sept.-Oct. 2003, doi: 10.1109/MEI.2003.1238713. keywords: Electrochemical impedance spectroscopy;Frequency domain analysis;Dielectrics and electrical insulation;Dielectric measurements;Frequency measurement;Time measure-

ment;Dielectric materials;Current measurement;Permittivity measurement;Gain measurement,

[25] Cigré Working Group D1.56, 2020, Field grading in electrical insulation systems, Technical Brochure 794

[26] T. Christen, L. Donzel and F. Greuter, "Nonlinear resistive electric field grading part 1: Theory and simulation," in IEEE Electrical Insulation Magazine, vol. 26, no. 6, pp. 47-59, November-December 2010, doi: 10.1109/MEI.2010.5599979. keywords: Finite element methods;Conductivity;Electric fields;Voltage control;Stress;Electrodes;Switches;electric stress control, nonlinear field grading material, finite element simulation;high voltage cable accessory,

[27] L. Donzel, F. Greuter and T. Christen, "Nonlinear resistive electric field grading Part 2: Materials and applications," in IEEE Electrical Insulation Magazine, vol. 27, no. 2, pp. 18-29, March-April 2011, doi: 10.1109/MEI.2011.5739419. keywords: Nonlinear systems;Electric fields;Conductivity;electric stress control;nonlinear field grading material;microvaristor,

[28] GIOVANNI MAAZZANTI, MASSIMO MARZINOTTO "Extruded cables for high voltage direct current transmission"

[29] L.A. Dissado and J.C. Fothergill, Edited by G.C. Stevens "Electrical Degradation and Breakdown in Polymers"

[30] N. A. Muhamad, B. T. Phung, T. R. Blackburn and K. X. Lai, "Polarization and Depolarization Current (PDC) tests on biodegradable and mineral transformer oils at different moisture levels," 2009 Australasian Universities Power Engineering Conference, Adelaide, SA, Australia, 2009, pp. 1-6. keywords: Polarization;Biodegradable materials;Minerals;Oil insulation;Moisture;Petroleum;Insulation testing;Conductivity;Power transformer insulation;Nondestructive testing;polarization current;depolarization current;biodegradable oil;mineral oil;insulation;mositure level,

[31] H. Shafi, T. M. Anthony, A. Basri, A. Raj and C. Chakrabarty, "Extraction of cable joints tangent delta from bulk tangent delta measurement using HFAC method," 2016 IEEE International Conference on Power and Energy (PECon), Melaka, Malaysia, 2016, pp. 306-310, doi: 10.1109/PECON.2016.7951578. keywords: Cable insulation;Dielectric losses;Voltage measurement;Power cables;Meters;tangent delta;cables joints;extraction method,

Department Of Electrical Engineering
Chalmers University Of Technology
Gothenburg, Sweden
www.chalmers.se

CHALMERS
UNIVERSITY OF TECHNOLOGY